

**Supporting information for:  
Design parameters for the 9,10-substituted  
anthracene chromophore and application in  
triplet-triplet annihilation photon upconversion**

Victor Gray,<sup>a</sup> Damir Dzebo,<sup>a</sup> Angelica Lundin,<sup>a</sup> Jonathan Alborzpour,<sup>a</sup>,  
Maria Abrahamsson,<sup>a</sup> Bo Albinsson,<sup>a</sup> and Kasper Moth-Poulsen<sup>a\*</sup>

<sup>a</sup>*Chalmers University of Technology, Gothenburg, Sweden*

E-mail: kasper.moth-poulsen@chalmers.se

---

\*To whom correspondence should be addressed

# Contents

1 UV/VIS absorption spectra	S2
2 Triplet Decay of Anthracene Derivatives	S7
3 Rate Equations governing TTA-UC	S12
4 Stern-Volmer quenching of PdOEP	S17
5 Freeze-Pumping procedure	S17
6 NMR Spectra of synthesized derivatives	S19

## 1 UV/VIS absorption spectra

Molar absorptivity of derivatives **1-10** are displayed in figure S1.

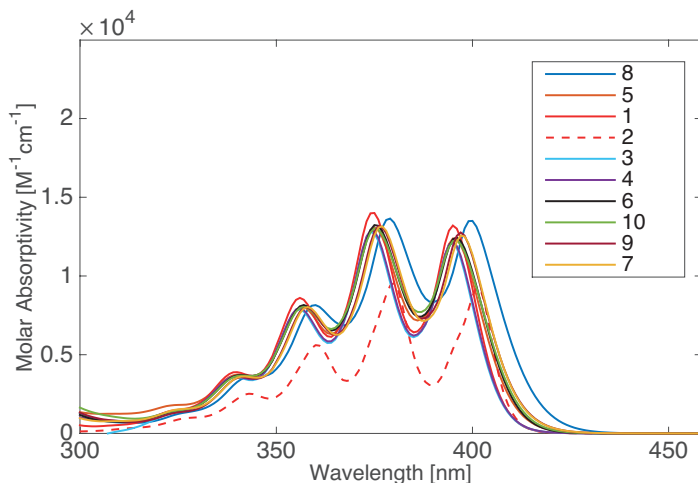


Figure S1: Molar absorptivity of derivatives **1-10**.

Normalized absorption of derivatives **1-10** at the solubility limit in toluene compared to absorption in solution is presented in figure S2-S11.

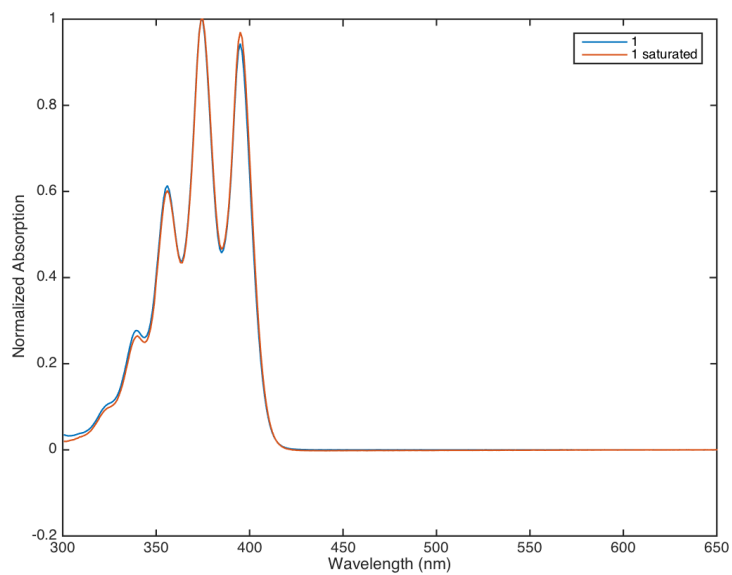


Figure S2: Absorption of **1** in solution and at saturation in toluene.

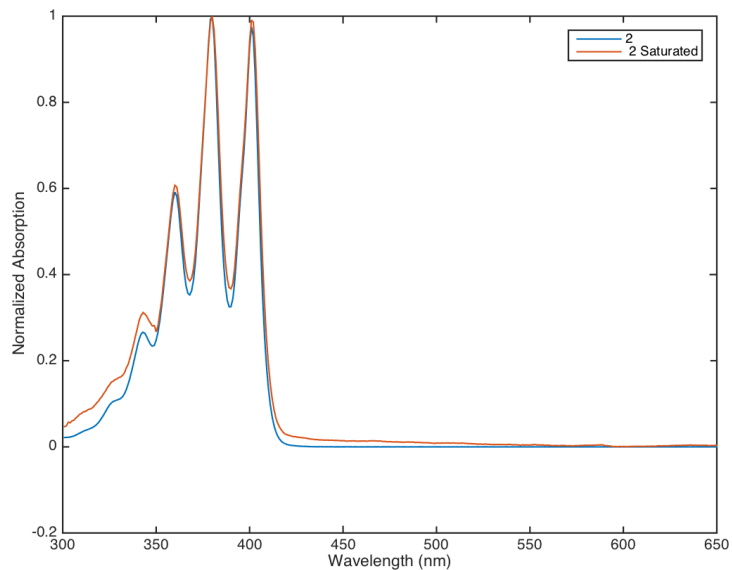


Figure S3: Absorption of **2** in solution and at saturation in toluene.

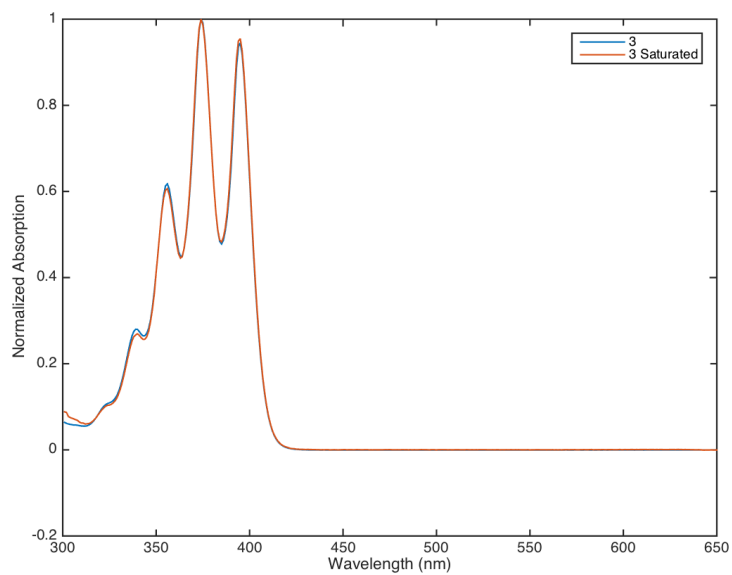


Figure S4: Absorption of **3** in solution and at saturation in toluene.

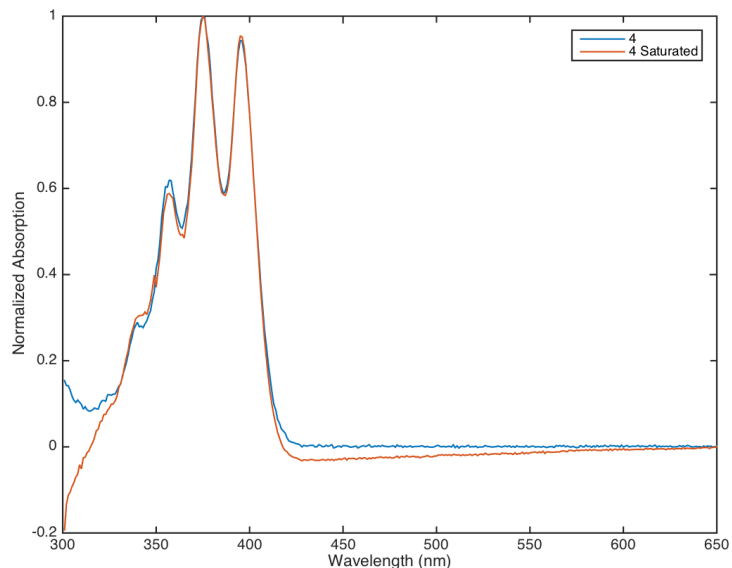


Figure S5: Absorption of **4** in solution and at saturation in toluene.

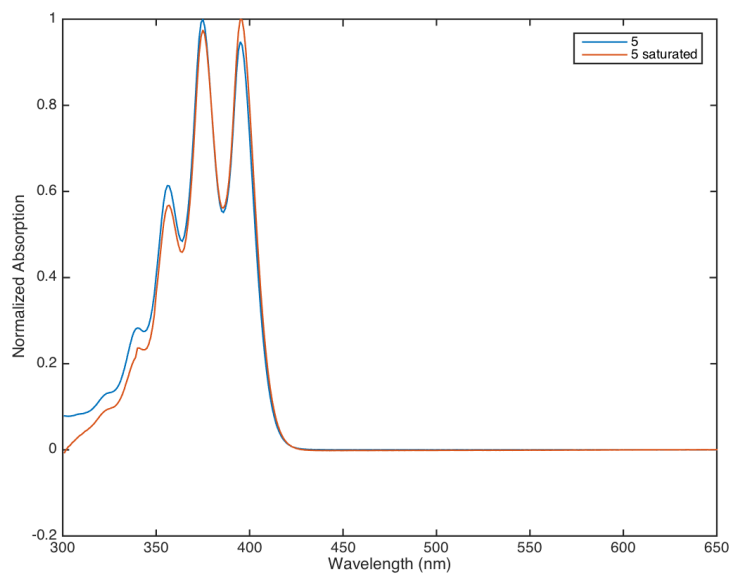


Figure S6: Absorption of **5** in solution and at saturation in toluene.

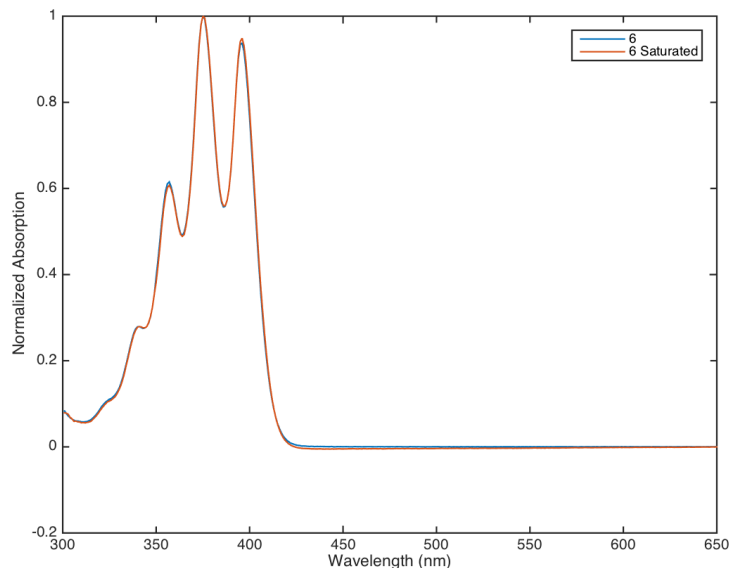


Figure S7: Absorption of **6** in solution and at saturation in toluene.

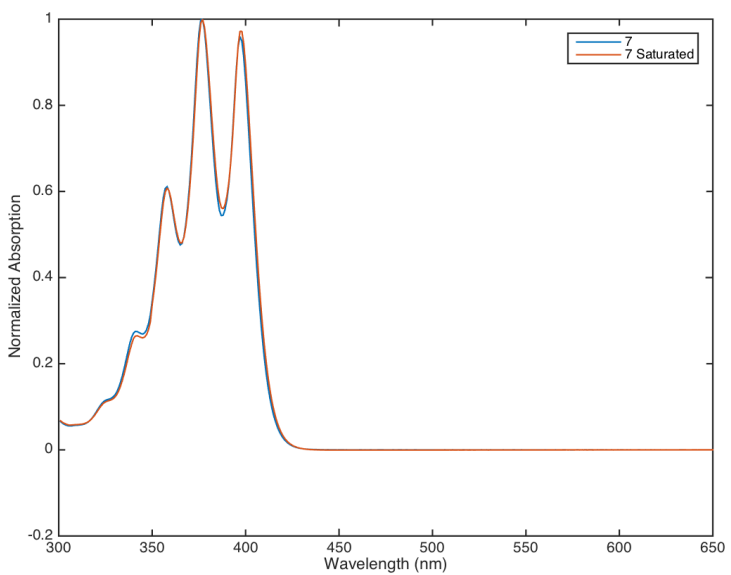


Figure S8: Absorption of **7** in solution and at saturation in toluene.

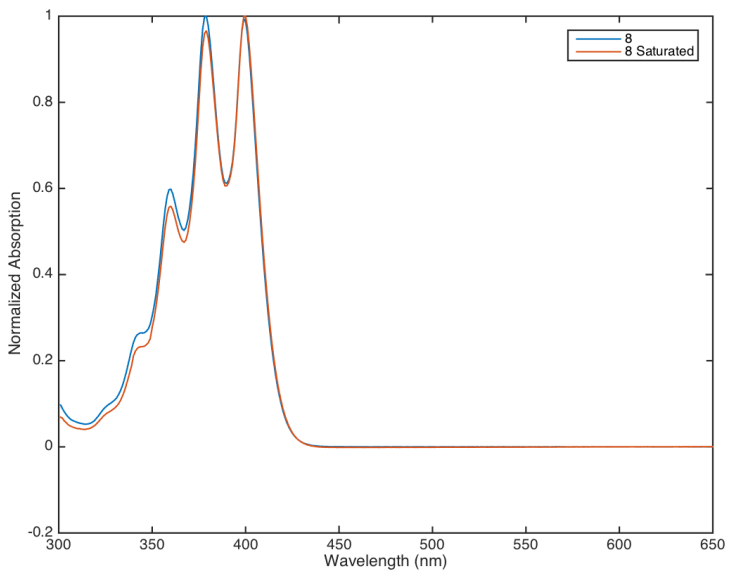


Figure S9: Absorption of **8** in solution and at saturation in toluene.

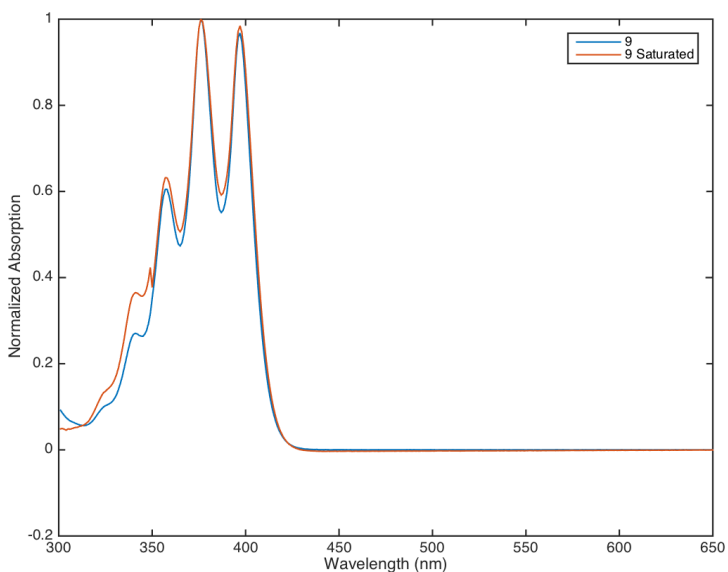


Figure S10: Absorption of **9** in solution and at saturation in toluene.

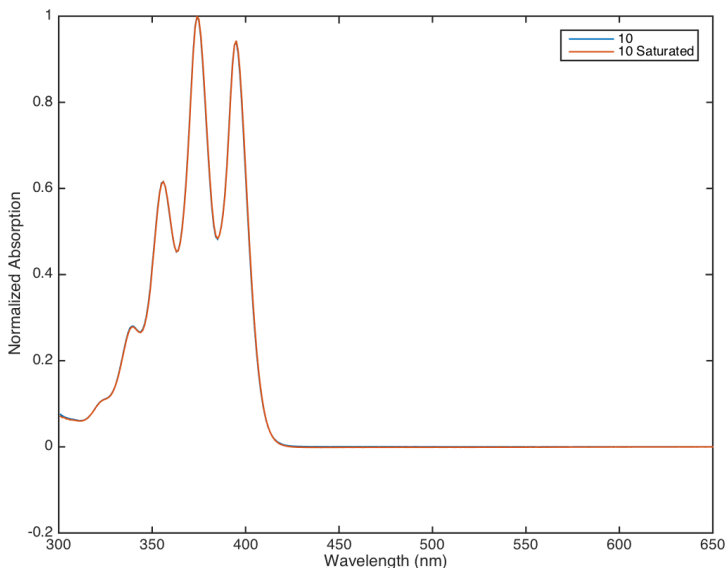


Figure S11: Absorption of **10** in solution and at saturation in toluene.

## 2 Triplet Decay of Anthracene Derivatives

Triplet state absorption decays of derivatives **1,3-10** are shown in figures S12-S20. Insets are residuals to the fit.

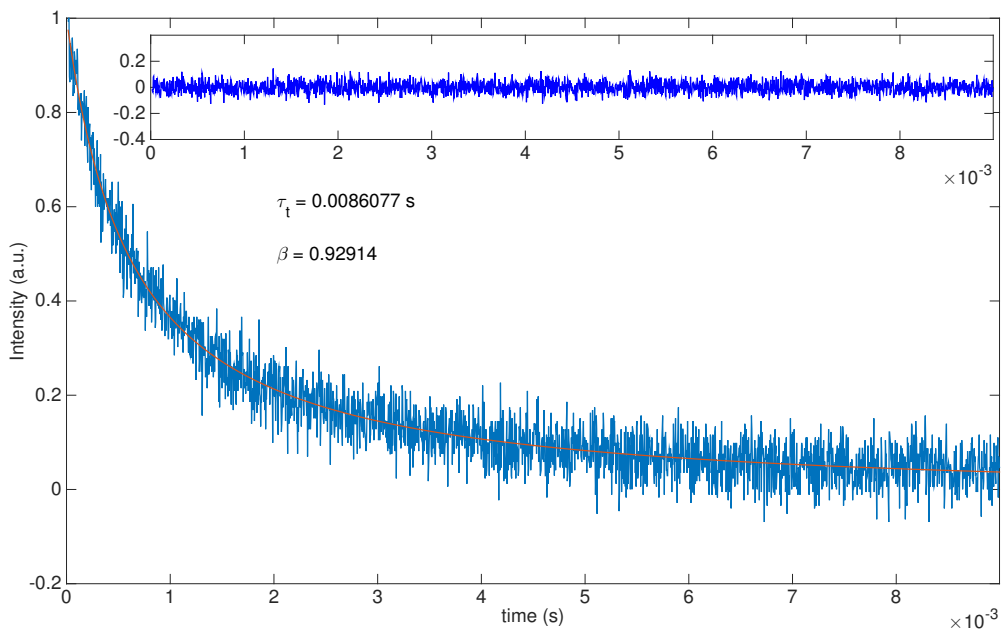


Figure S12: Transient absorption decay of **1** at 452 nm corresponding to the triplet excited state

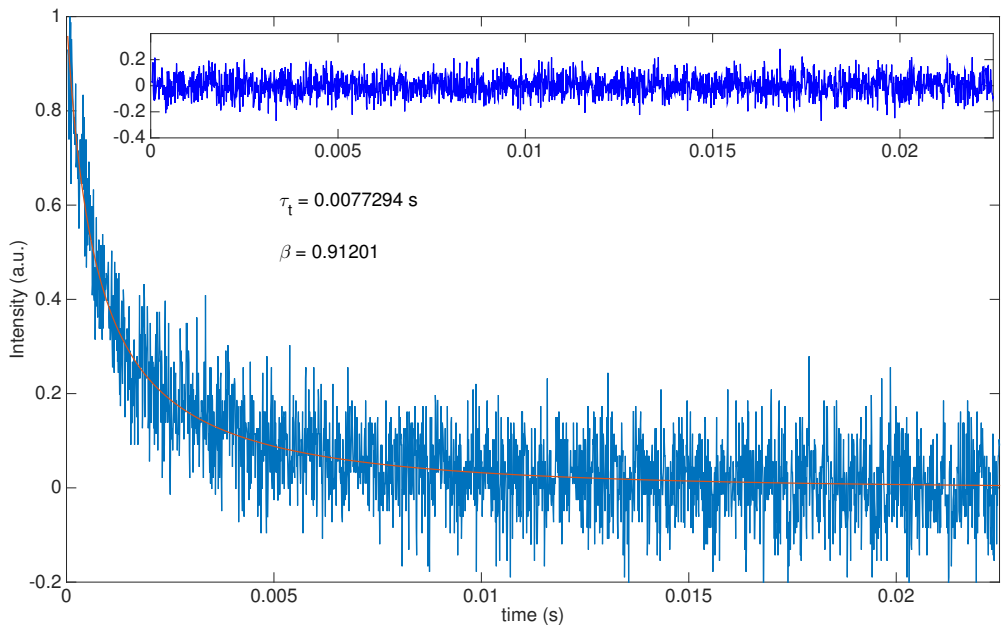


Figure S13: Transient absorption decay of **3** at 452 nm corresponding to the triplet excited state

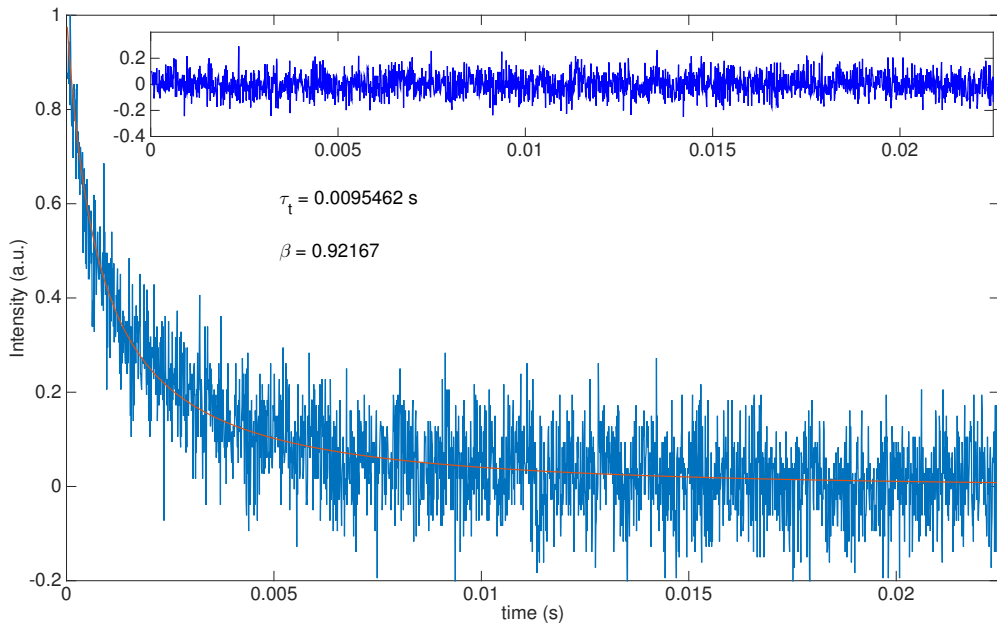


Figure S14: Transient absorption decay of **4** at 452 nm corresponding to the triplet excited state

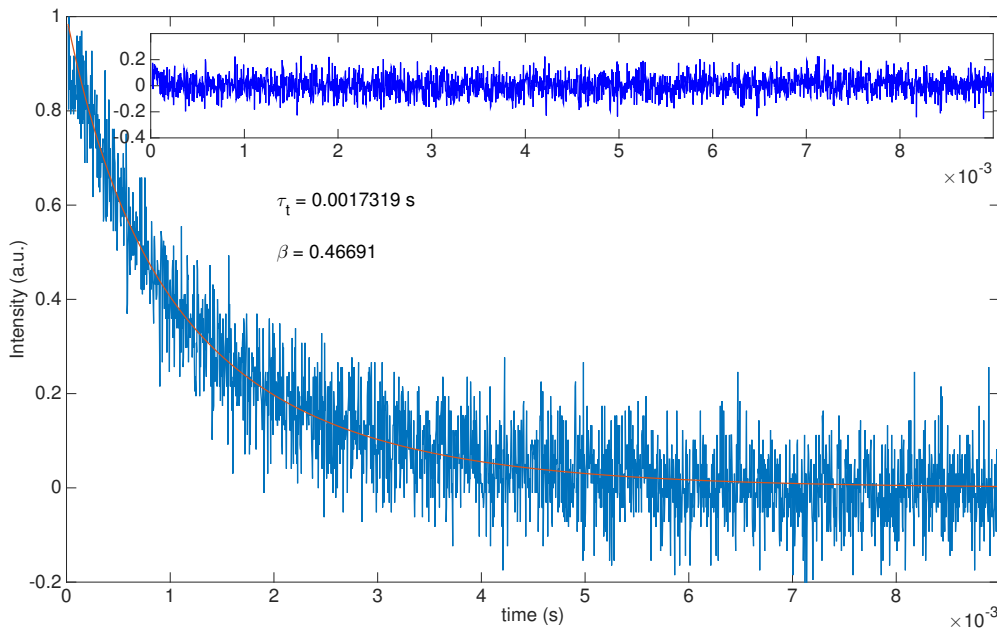


Figure S15: Transient absorption decay of **5** at 452 nm corresponding to the triplet excited state

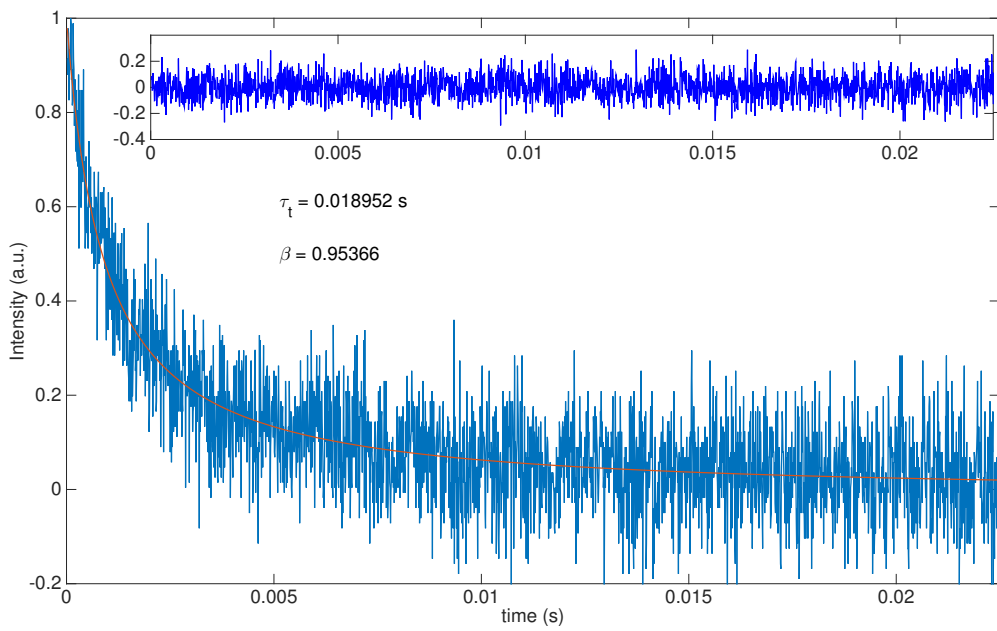


Figure S16: Transient absorption decay of **6** at 452 nm corresponding to the triplet excited state

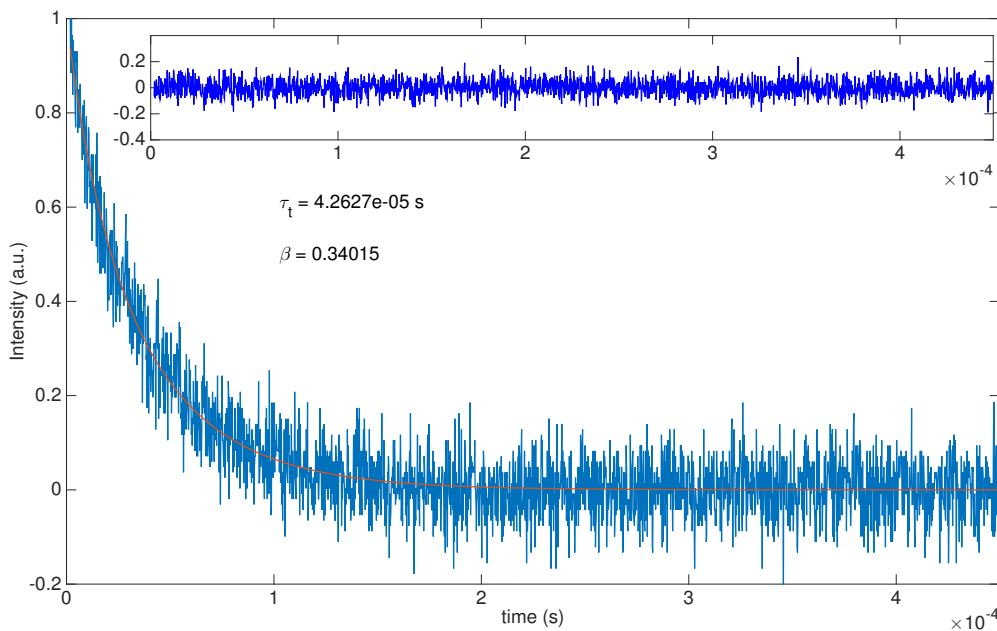


Figure S17: Transient absorption decay of **7** at 452 nm corresponding to the triplet excited state

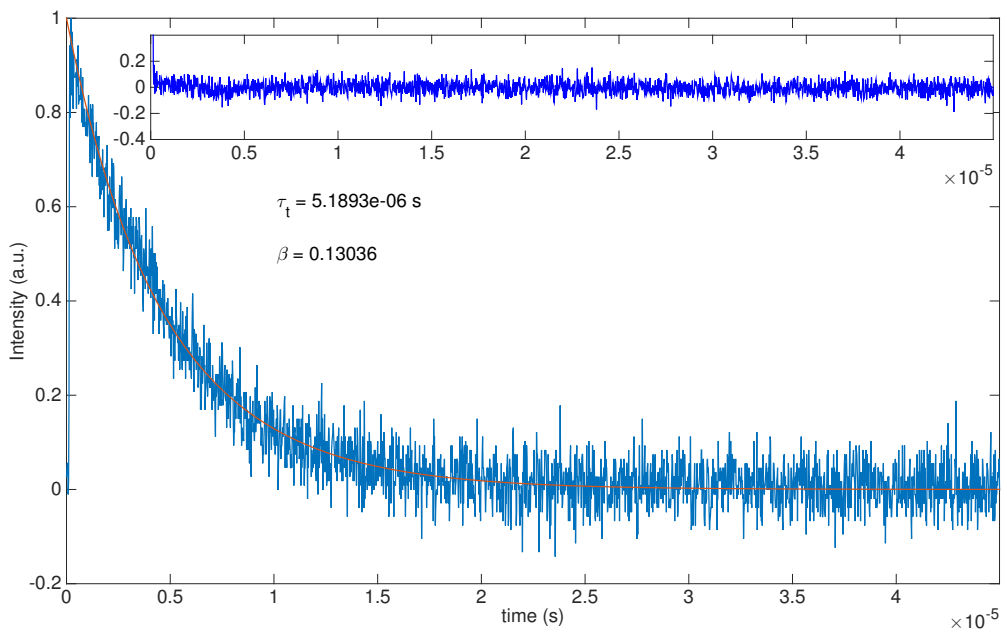


Figure S18: Transient absorption decay of **8** at 452 nm corresponding to the triplet excited state

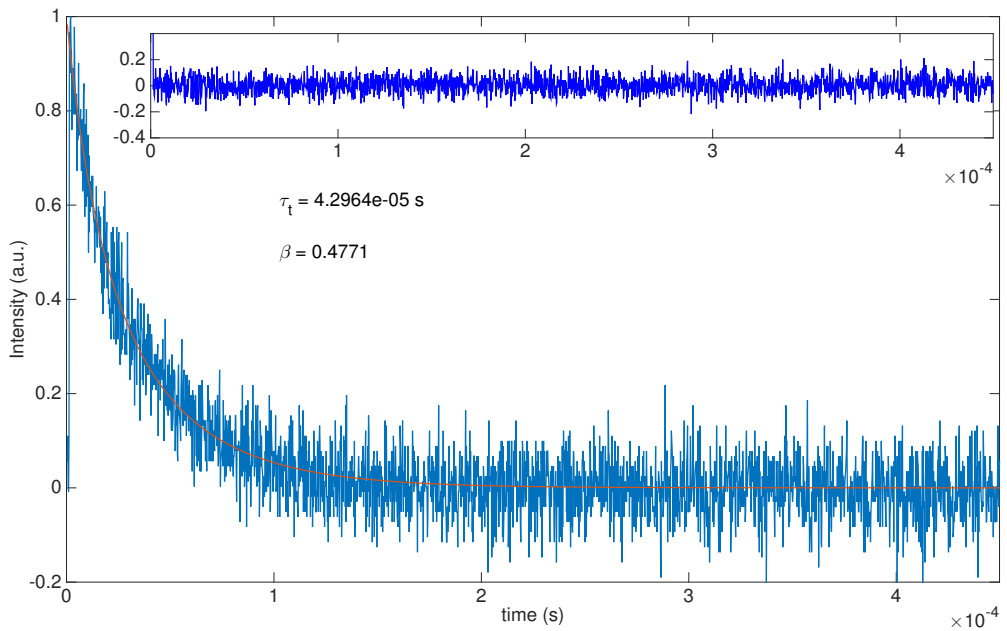


Figure S19: Transient absorption decay of **9** at 452 nm corresponding to the triplet excited state

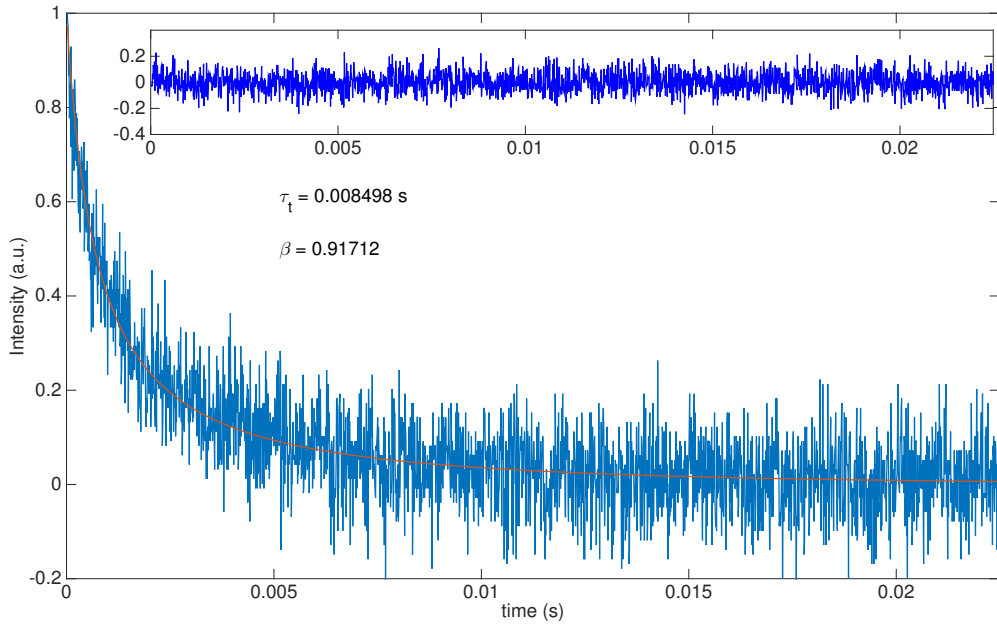


Figure S20: Transient absorption decay of **10** at 452 nm corresponding to the triplet excited state

### 3 Rate Equations governing TTA-UC

Assuming that on the timescale of the experiment the laser pulse, the absorption of the sensitizer and the following intersystem crossing to the triplet state is instantaneous and that the sensitizer concentration is low enough that no triplet-triplet annihilation occurs between sensitizer molecules or sensitizer and annihilator molecules the rate equations governing the triplet-triplet annihilation system are:<sup>S1</sup>

$$\frac{d[{}^3S^*]}{dt} = -k_{TET}[{}^3S^*][{}^1A] \quad (1)$$

$$\frac{d[{}^3A^*]}{dt} = k_{TET}[{}^3S^*][{}^1A] - 2k_{TTA}[{}^3A^*]^2 - k_{PA}[{}^3A^*] \quad (2)$$

$$\frac{d[{}^1A^*]}{dt} = k_{TTA}[{}^3A^*]^2 - k_F[{}^1A^*] \quad (3)$$

$$\frac{d[{}^0A]}{dt} = -k_{TET}[{}^3S^*][{}^1A] + k_{TTA}[{}^3A^*]^2 + k_F[{}^1A^*] \quad (4)$$

where  $[{}^3S^*]$  and  $[{}^3A^*]$  are the sensitizer and annihilator triplet concentrations respectively. Correspondingly  $[{}^1A^*]$  and  $[{}^1A]$  are the concentrations of annihilator in the excited singlet and ground state respectively. In reality one TTA event does not necessarily form a singlet state if triplet and quintet states are energetically accessible, and spin-statistics was first assumed to limit the TTA process to efficiencies below 1/9. However experimental data has disproven this limit with observed efficiencies well above 1/9.<sup>S2,S3</sup> Unfortunately a full theoretical prediction of the actual limit for TTA systems is still lacking. Therefore we have, like others,<sup>S4</sup> chosen not to consider spin-statistics in the above rate equations.

Initial triplet concentration of the sensitizer  $[{}^3S^*]$  is estimated from the ground state bleach at 540 nm. At 410 nm three features are observed over the time period of data recording; the annihilator triplet absorption together with the sensitizer triplet absorption are first observed as a positive feature in the transient, this is followed by a change to a negative feature as the emission from the annihilator singlet state rises due to TTA, this is as expected for a TTA-UC system. Therefore the recorded transient at 410 nm has to be fitted to equation 5:

$$\Delta A_{410nm} = \Delta\epsilon_{AT} \times [{}^3A^*] + \Delta\epsilon_{ST} \times [{}^3S^*] - a_{FL} \times [{}^1A^*]. \quad (5)$$

Where  $\Delta\epsilon_{AT}$  and  $\Delta\epsilon_{ST}$  are the differential absorptivity of the annihilator and sensitizer respectively, taking into account the triplet state absorption and ground state bleach.  $a_{FL}$  is a scaling factor for the fluorescence intensity of the annihilator. At 650 nm only the sensitizer emission is observed and the decay is fitted to equation 6:

$$\Delta A_{650nm} = -a_{Phos} \times [{}^3S^*]. \quad (6)$$

where  $a_{Phos}$  is a scaling factor for the sensitizer phosphorescence intensity. Differential equations 1-4 are solved using MATLAB's ODE solver ode23s. The obtained concentrations at defined time intervals are then used in equations 5 and 6 and the results are

compared to the obtained data at 410 nm (0.1-5  $\mu$ s and 0.0001-1 ms) and 650 nm (0.1-5  $\mu$ s) simultaneously. The difference is minimized using the fmincon function in MATLAB. Due to limited time resolution of the laser setup and detection system fits were performed beyond the first 100 ns of the transients.

Plots of fitted transients are displayed in figures S21-S25. In these figures the top graph shows the transient at 410 nm and the fit to equation 5, the inset shows the fit to equation 5 between 0-5  $\mu$ s as well as the decay at 650 nm and the corresponding fit to equation 6.

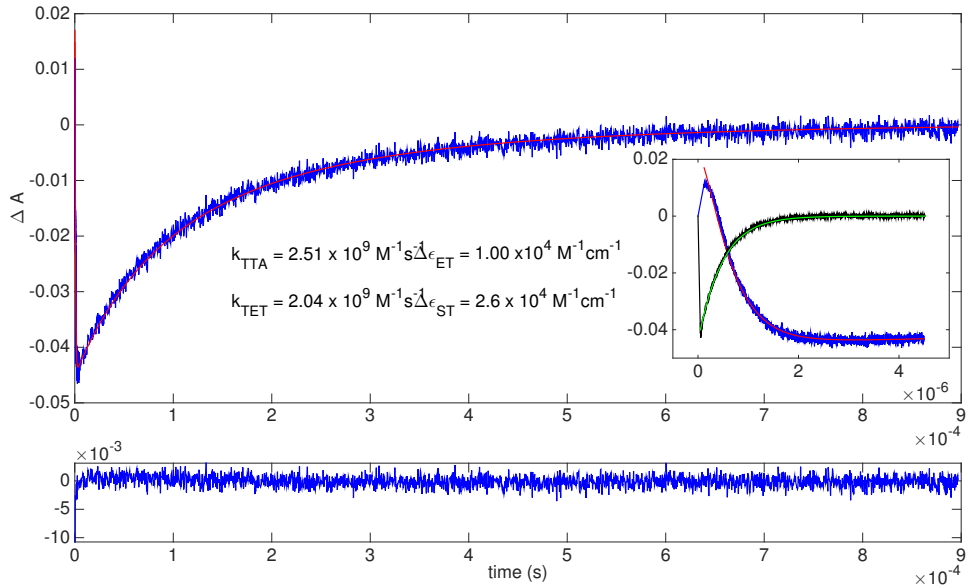


Figure S21: Transient absorption measurements of **1**(1 mM) and **PtOEP**(3.4  $\mu$ M) at 410 nm (Emitter Decay, blue) and 650 nm (Sensitizer decay, black) and respective fits of equations 5 and 6 to the decays. Bottom panel shows the residual of the fitted annihilator decay.

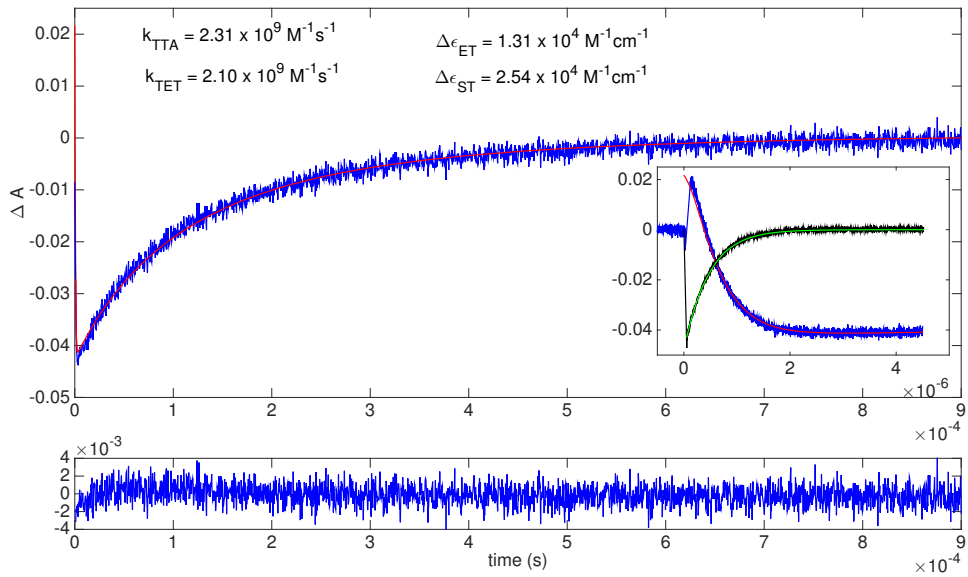


Figure S22: Transient absorption measurements of **3**(1 mM) and **PtOEP**(3.4 $\mu$ M) at 410 nm (Emitter Decay, blue) and 650 nm (Sensitizer decay, black) and respective fits of equations 5 and 6 to the decays. Bottom panel shows the residual of the fitted annihilator decay

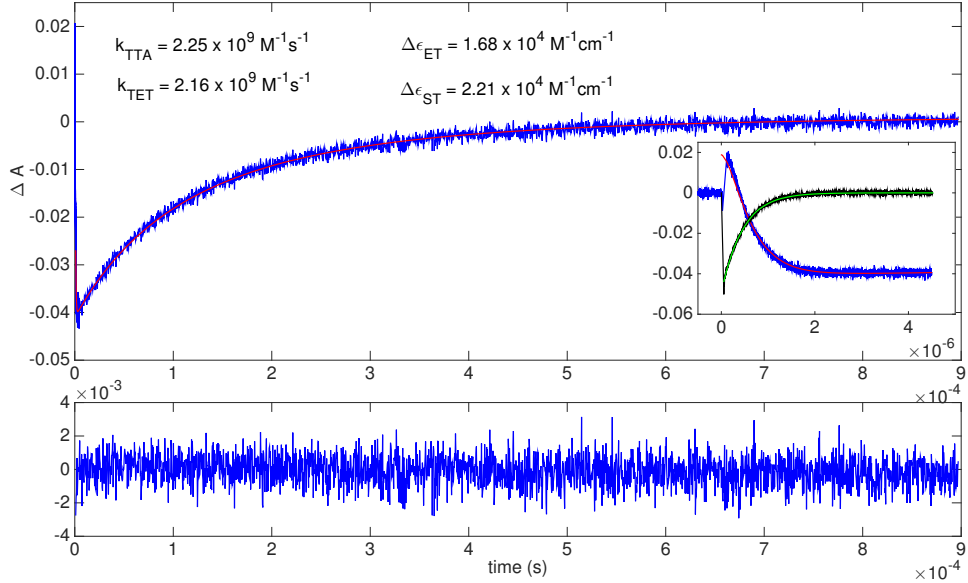


Figure S23: Transient absorption measurements of **4** (1 mM) and **PtOEP** (3.4 $\mu$ M) at 410 nm (Emitter Decay, blue) and 650 nm (Sensitizer decay, black) and respective fits of equations 5 and 6 to the decays. Bottom panel shows the residual of the fitted annihilator decay

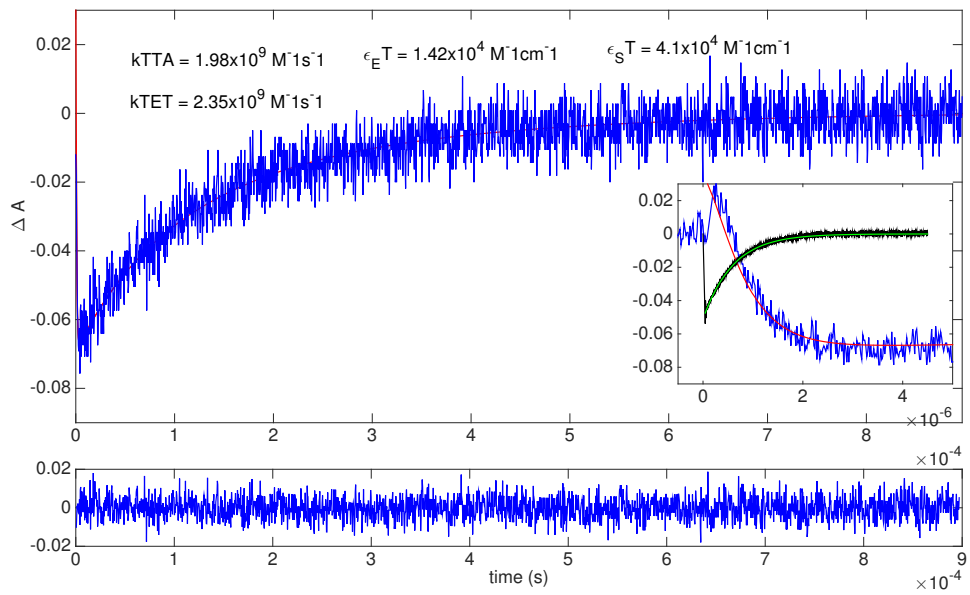


Figure S24: Transient absorption measurements of **5**(0.67 mM) and **PtOEP**(3.4 μM) at 410 nm (Emitter Decay, blue) and 650 nm (Sensitizer decay, black) and respective fits of equations 5 and 6 to the decays. Bottom panel shows the residual of the fitted annihilator decay

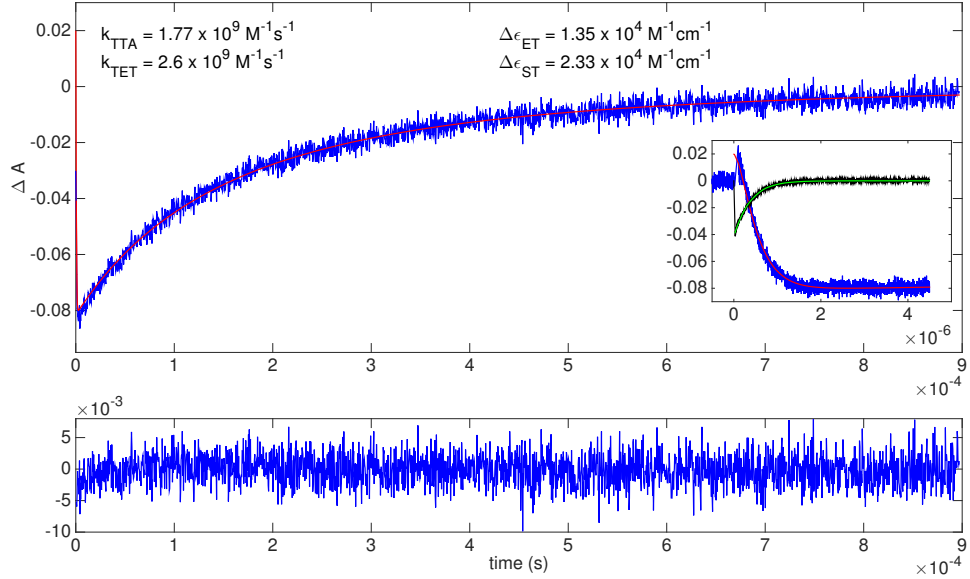


Figure S25: Transient absorption measurements of **10**(1 mM) and **PtOEP**(3.4 μM) at 410 nm (Emitter Decay, blue) and 650 nm (Sensitizer decay, black) and respective fits of equations 5 and 6 to the decays. Bottom panel shows the residual of the fitted annihilator decay

## 4 Stern-Volmer quenching of PdOEP

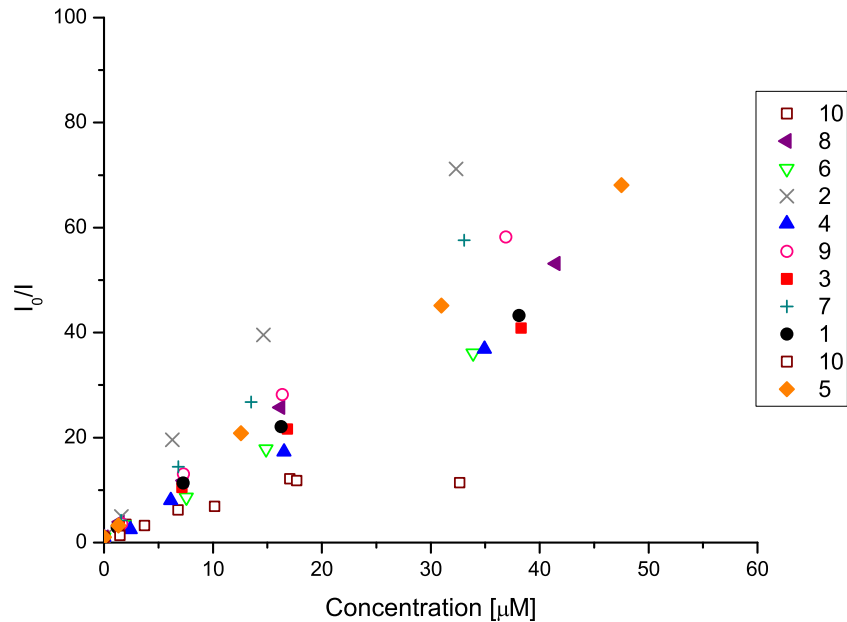


Figure S26: Stern-Volmer plot of PdOEP quenching by derivatives **1-10**

## 5 Freeze-Pumping procedure

The following procedure was followed for degassing the UC-samples:

1. Freeze the Sample
2. Pump to  $P < 1\text{E}-4$  mbar
3. Close
4. Thaw
5. Close
6. Repeat 1-2
7. Refill the frozen sample with Nitrogen
8. Pump to  $P < 1\text{E}-4$  mbar
9. Repeat Steps 3-8 two times
10. Close
11. Thaw
12. Refill with nitrogen
13. Repeat steps 1-8
14. Repeat steps 3-8 once
15. Repeat steps 10-12
16. Repeat steps 1-8
17. Repeat steps 10-11

18. Repeat steps 1-2
19. With the sample still in liquid nitrogen seal the sample with a Propane-Butane mixed gas burner.

## 6 NMR Spectra of synthesized derivatives

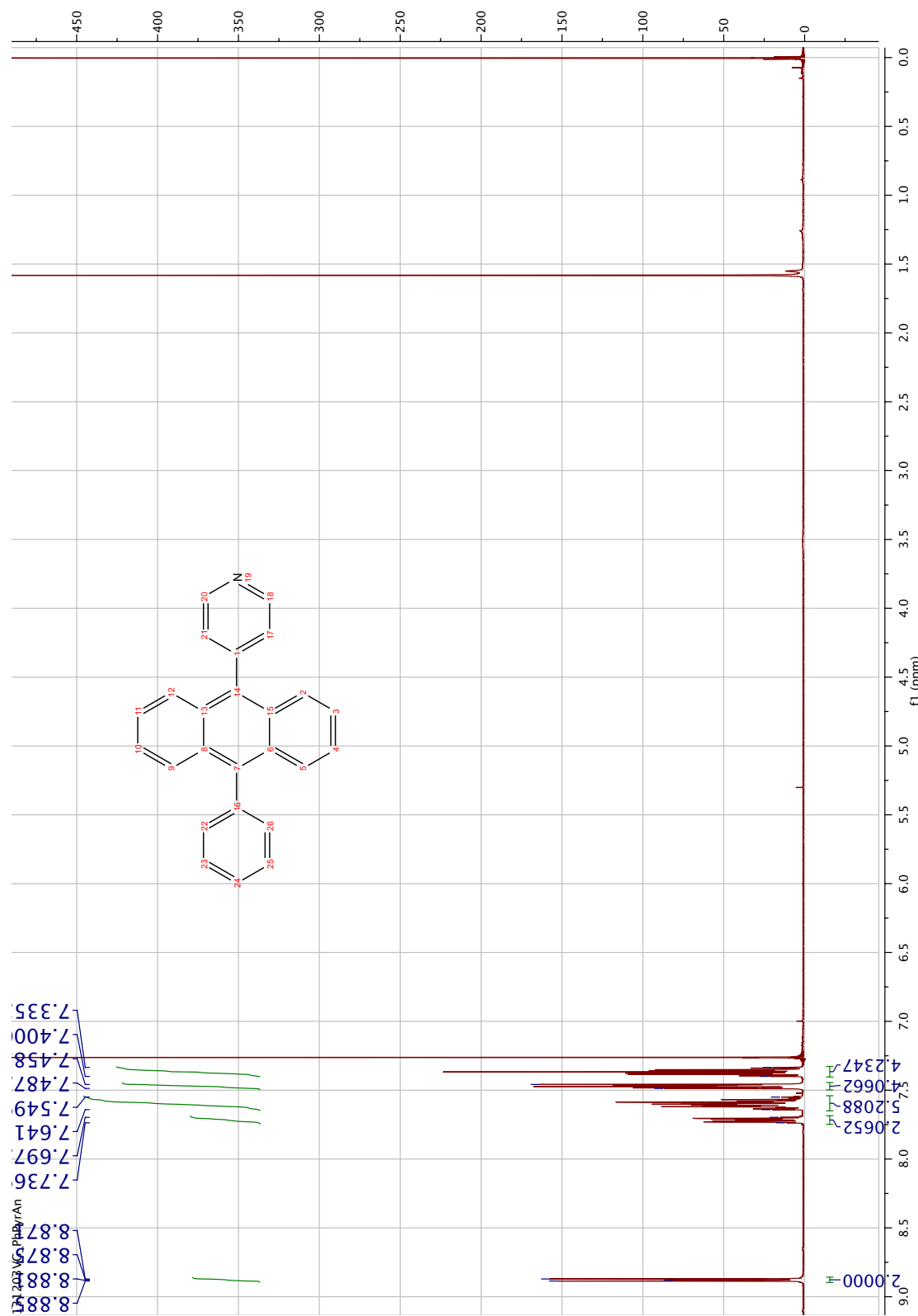


Figure S27:  $^1\text{H}$ -NMR of **3**

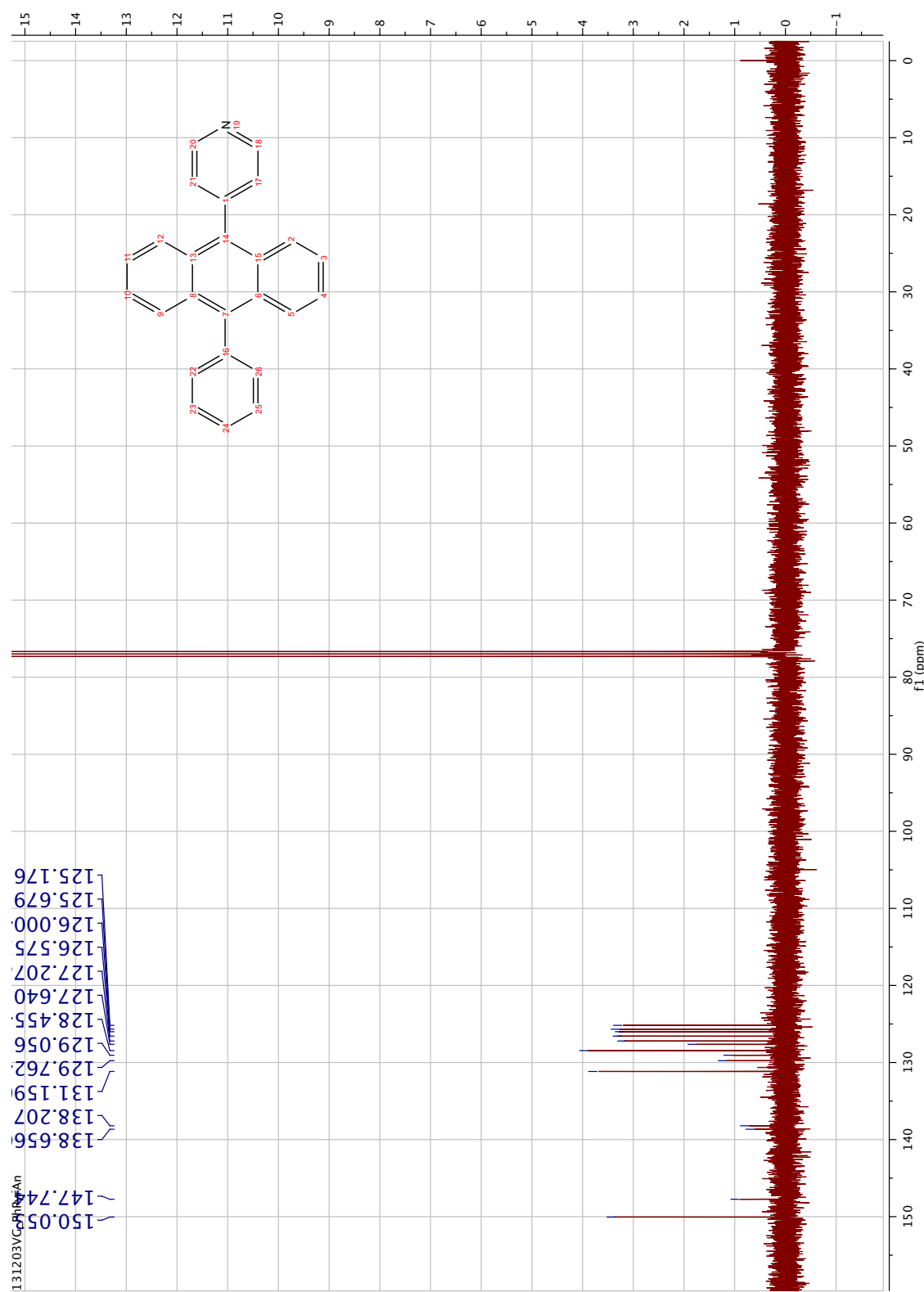


Figure S28:  $^{13}\text{C}$ -NMR of **3**

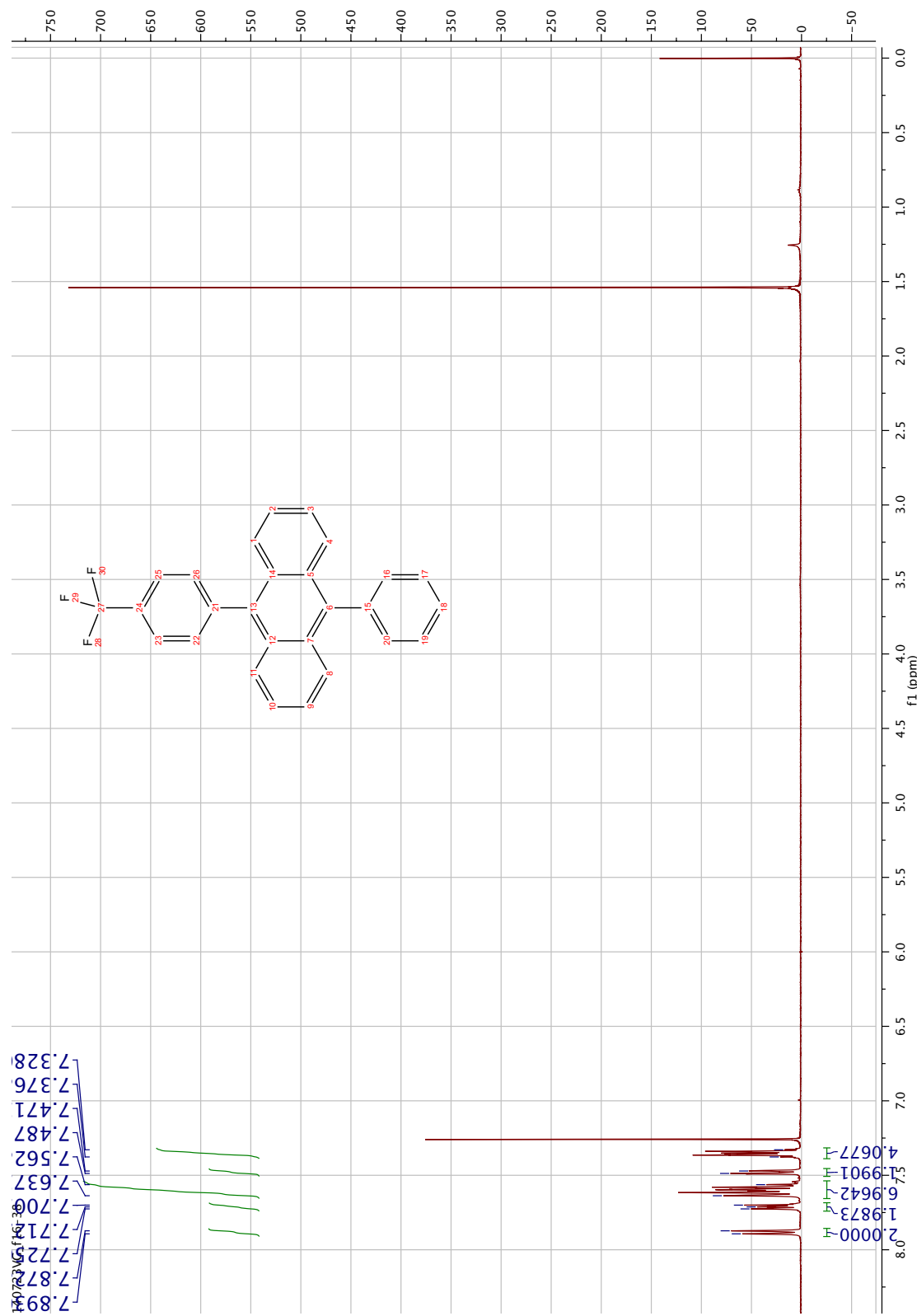
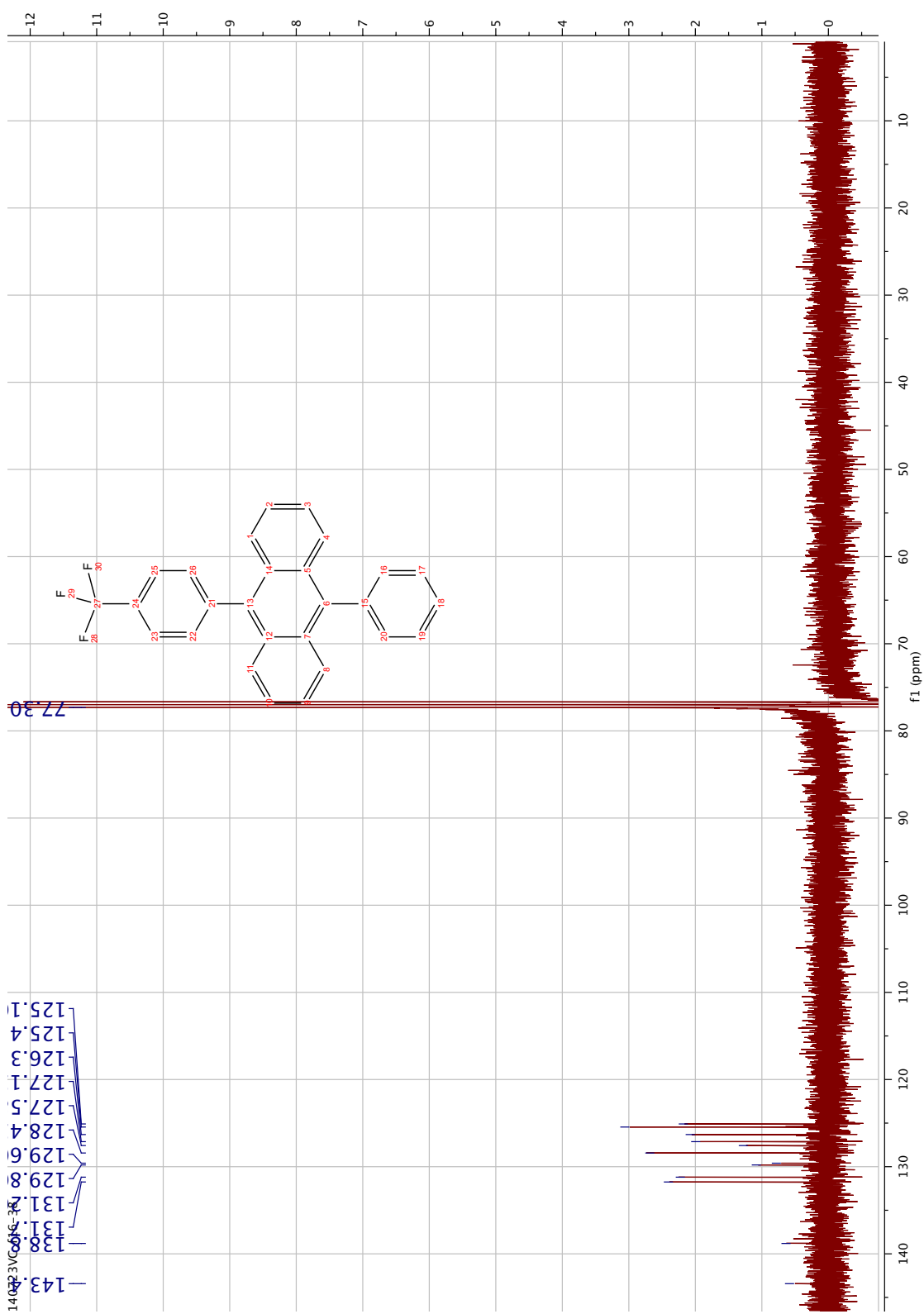


Figure S29:  $^1\text{H}$ -NMR of 4



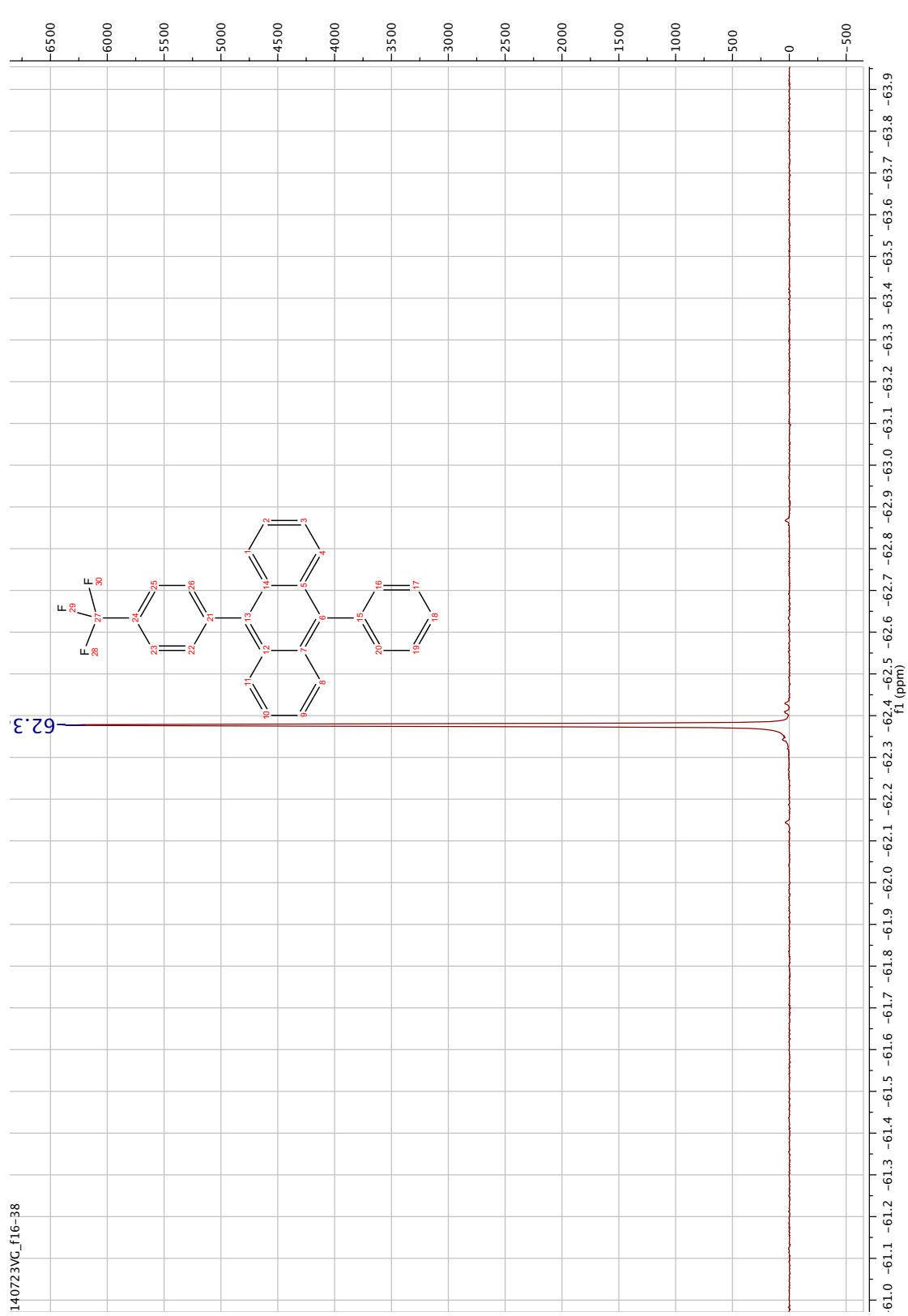


Figure S31:  $^{19}\text{F}$ -NMR of **4**

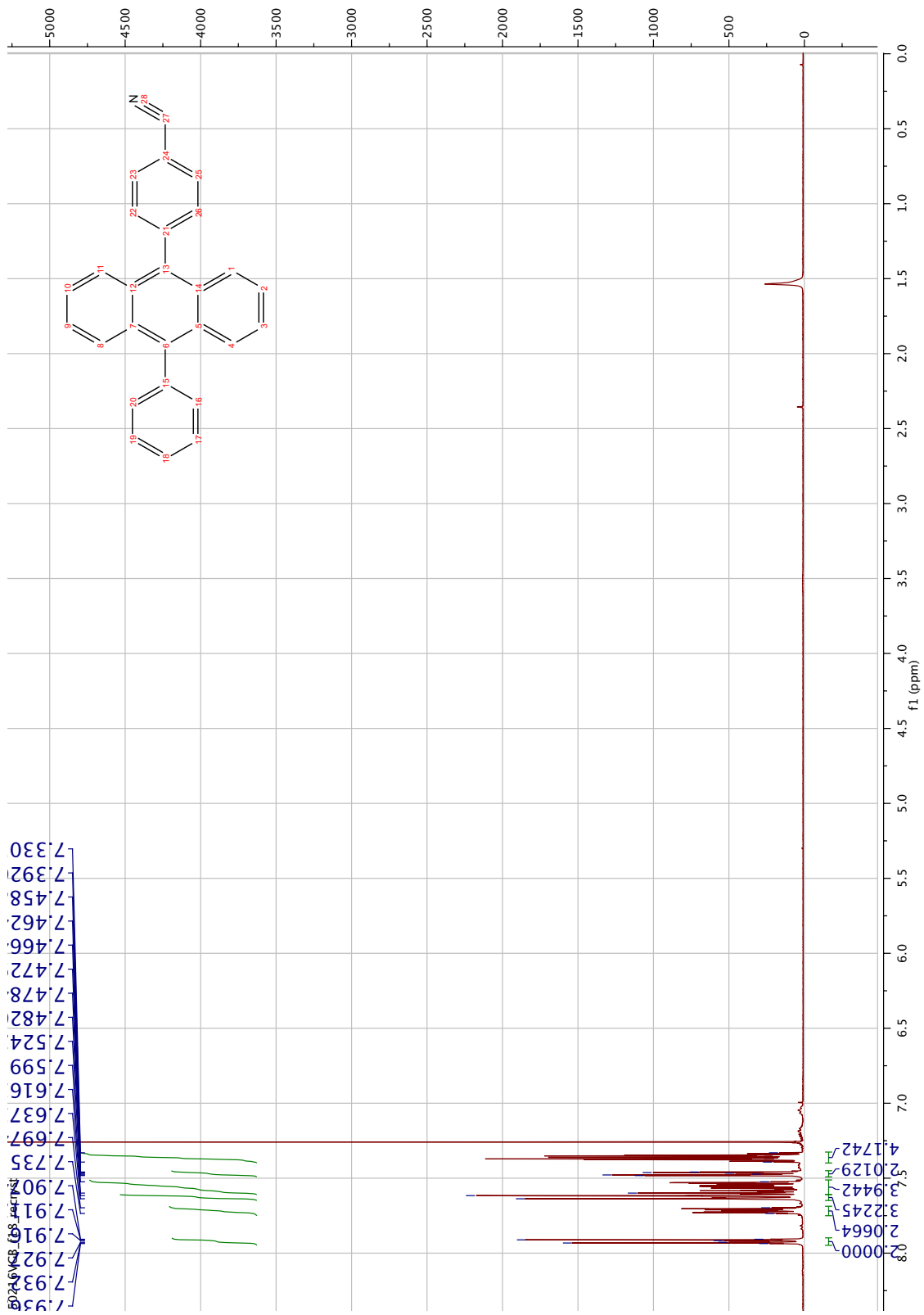


Figure S32:  $^1\text{H}$ -NMR of **5**

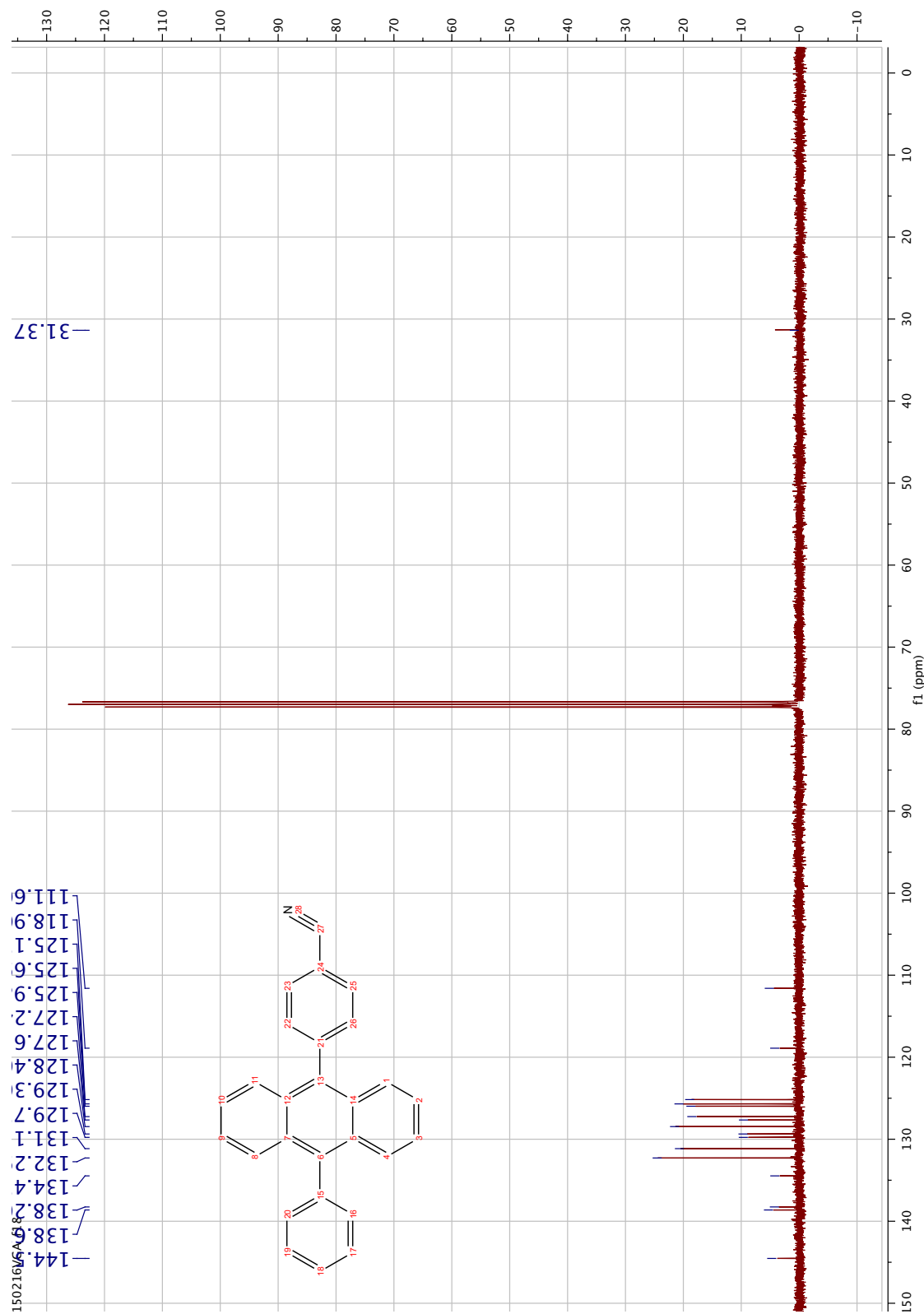


Figure S33:  $^{13}\text{C}$ -NMR of **5**

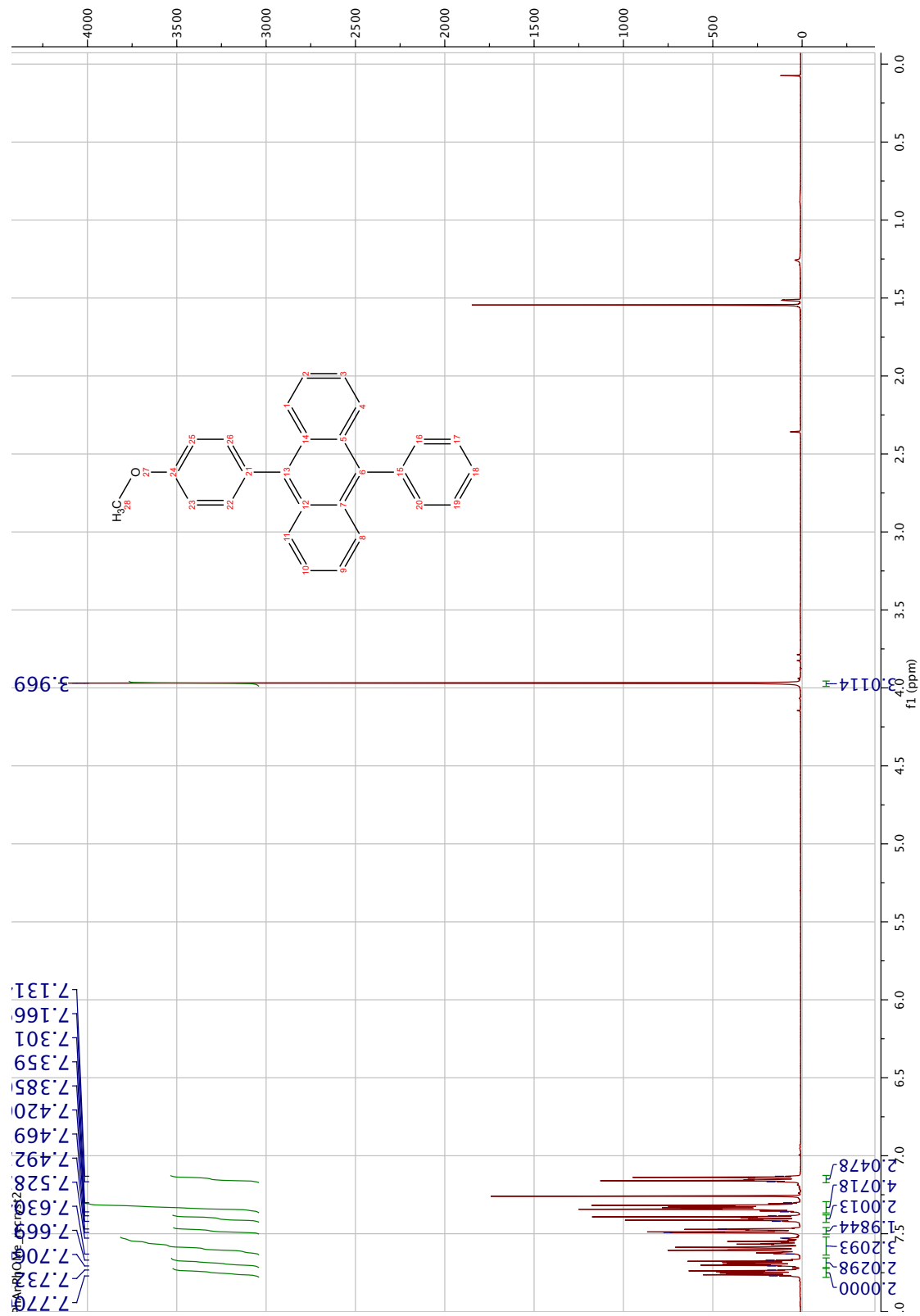


Figure S34:  $^1\text{H}$ -NMR of **6**

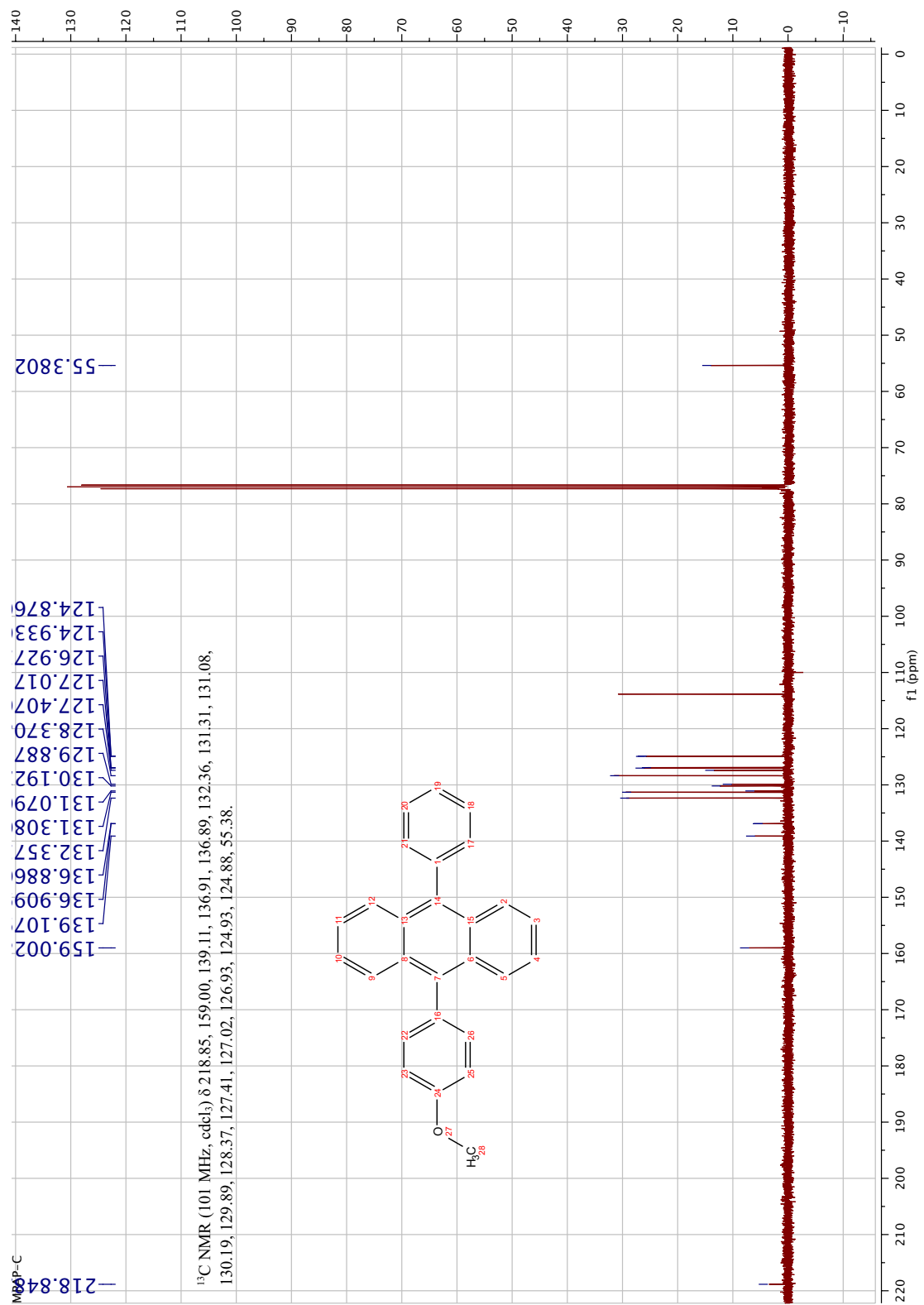


Figure S35:  $^{13}\text{C}$ -NMR of **6**

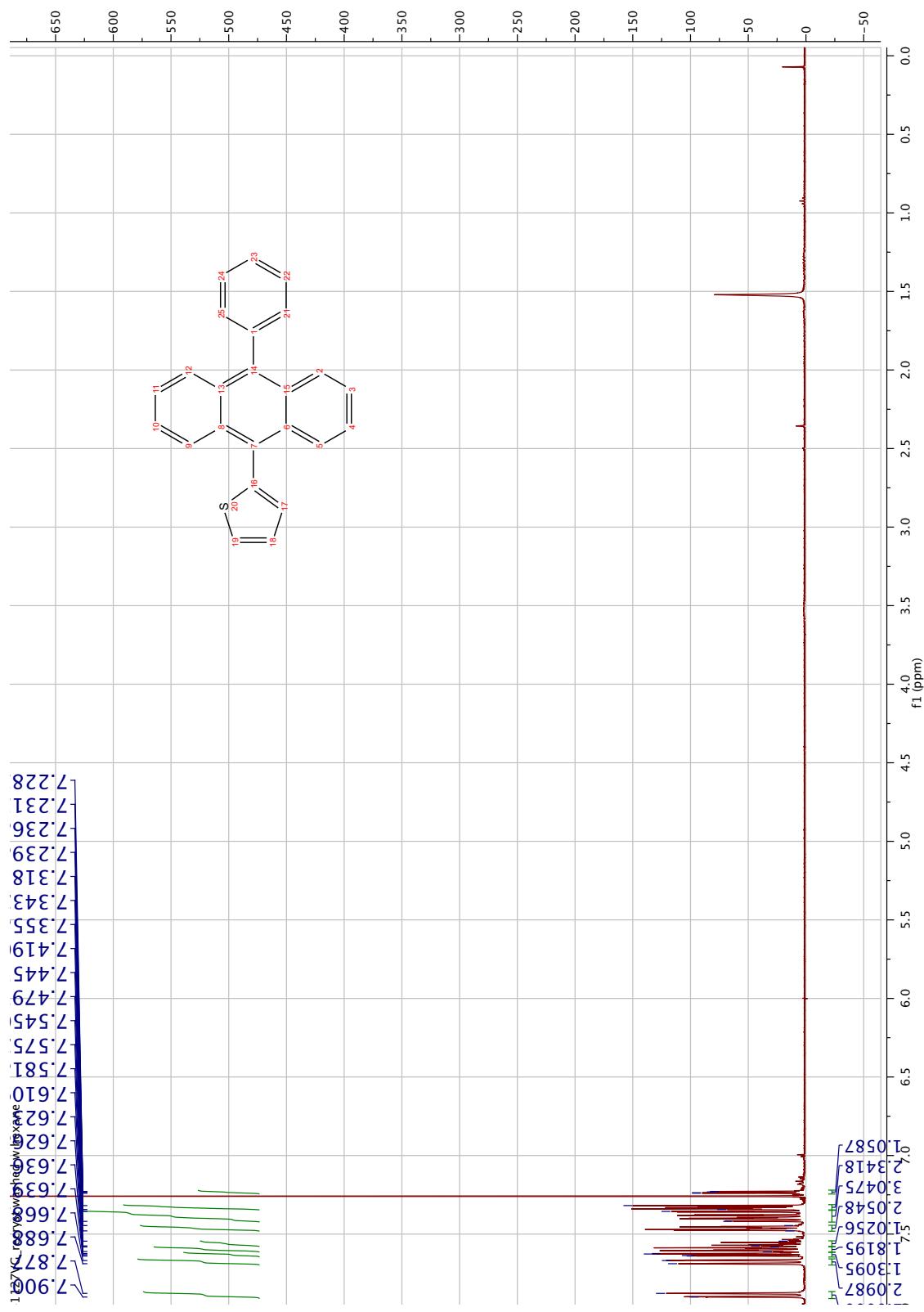


Figure S36:  $^1\text{H}$ -NMR of **7**

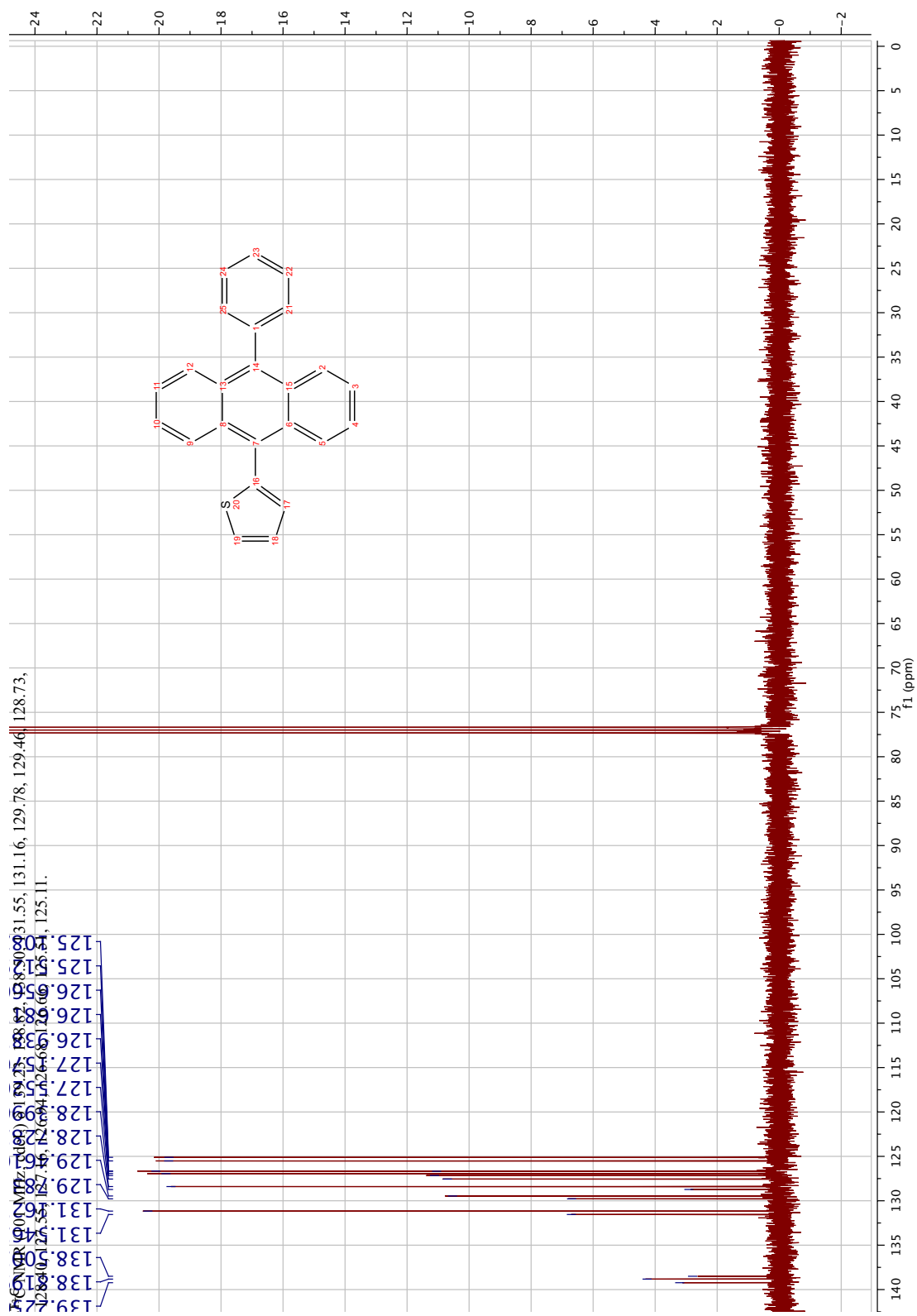


Figure S37:  $^{13}\text{C}$ -NMR of **7**

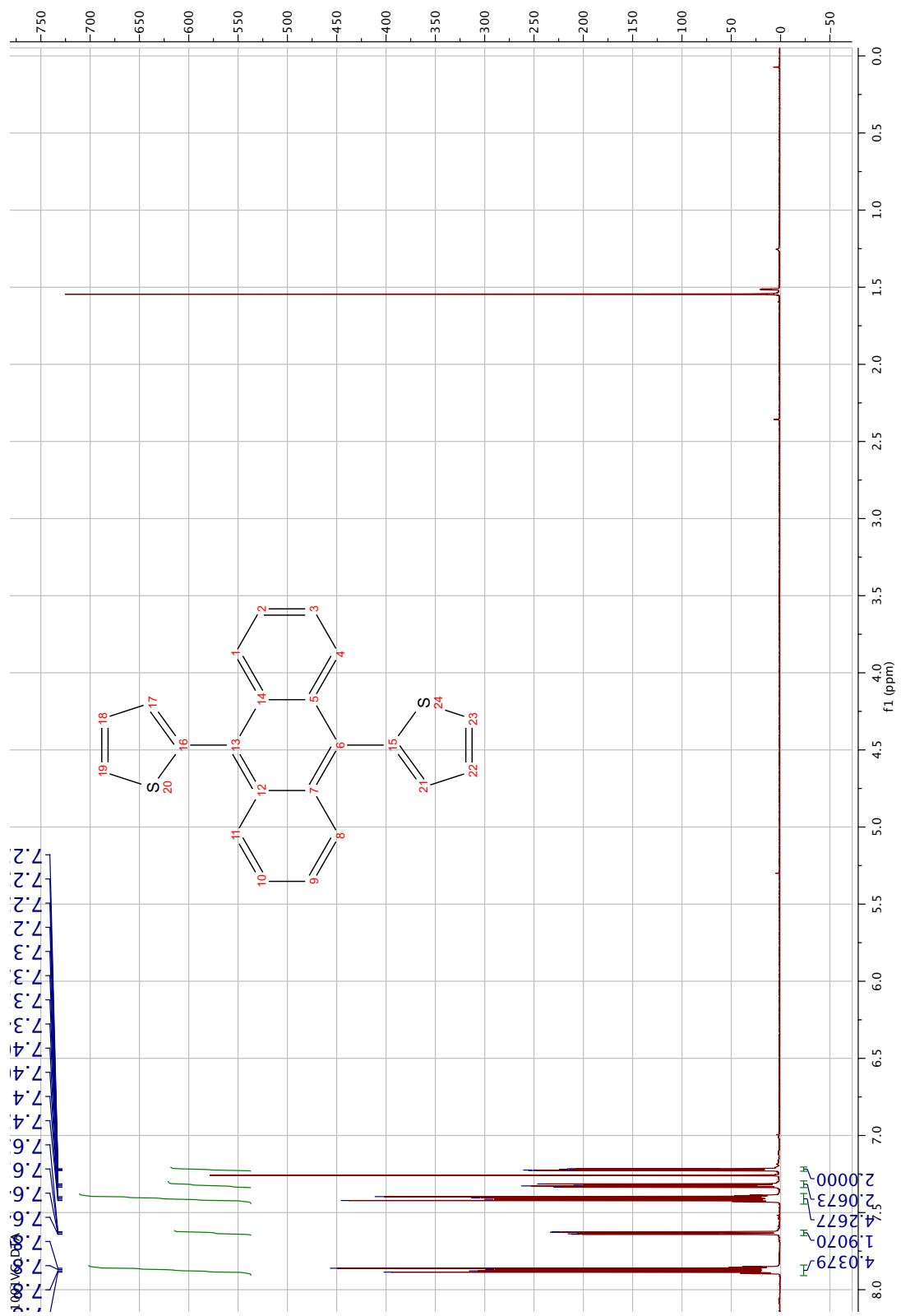


Figure S38:  $^{13}\text{C}$ -NMR of 8

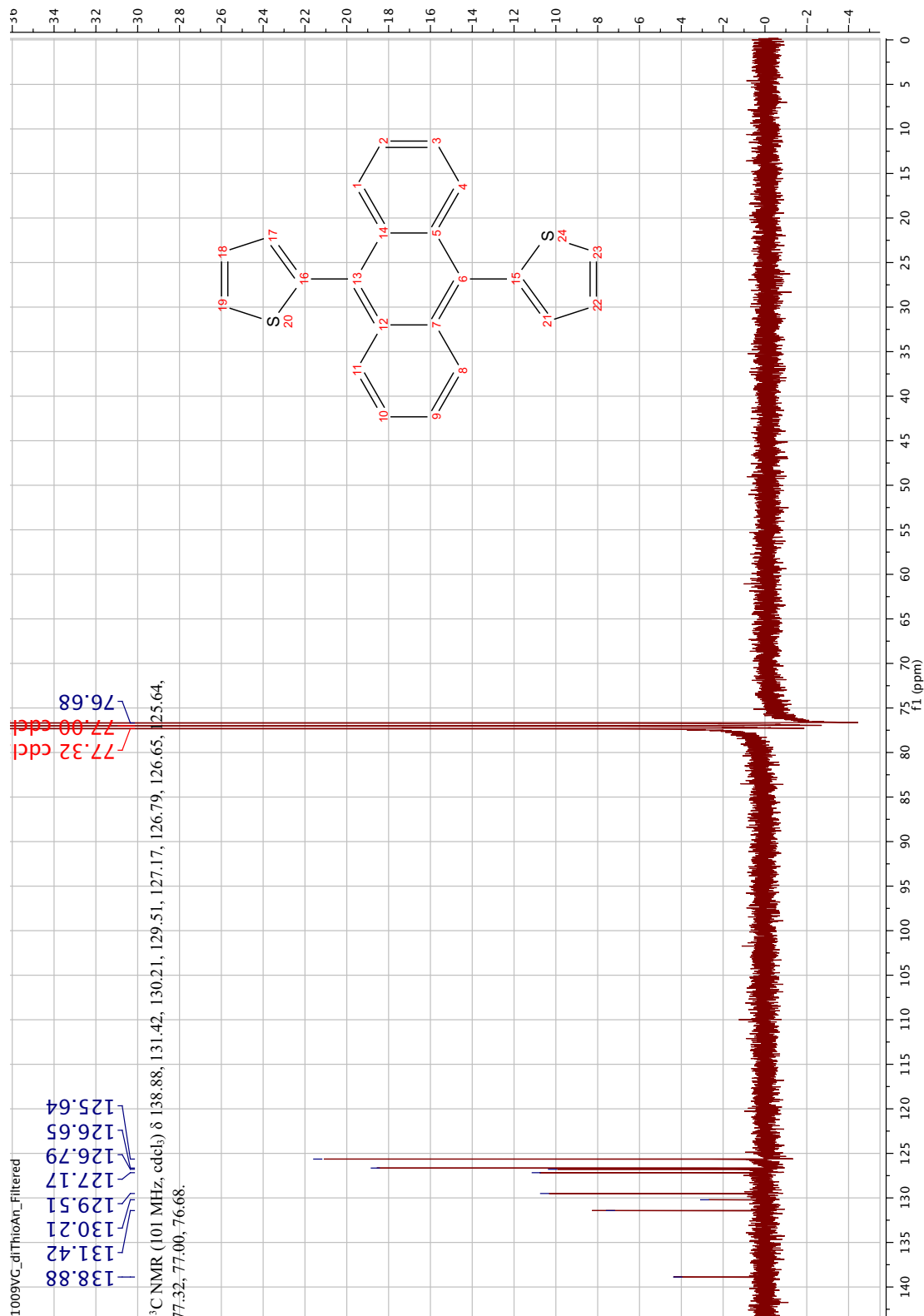


Figure S39: <sup>13</sup>C-NMR of **8**

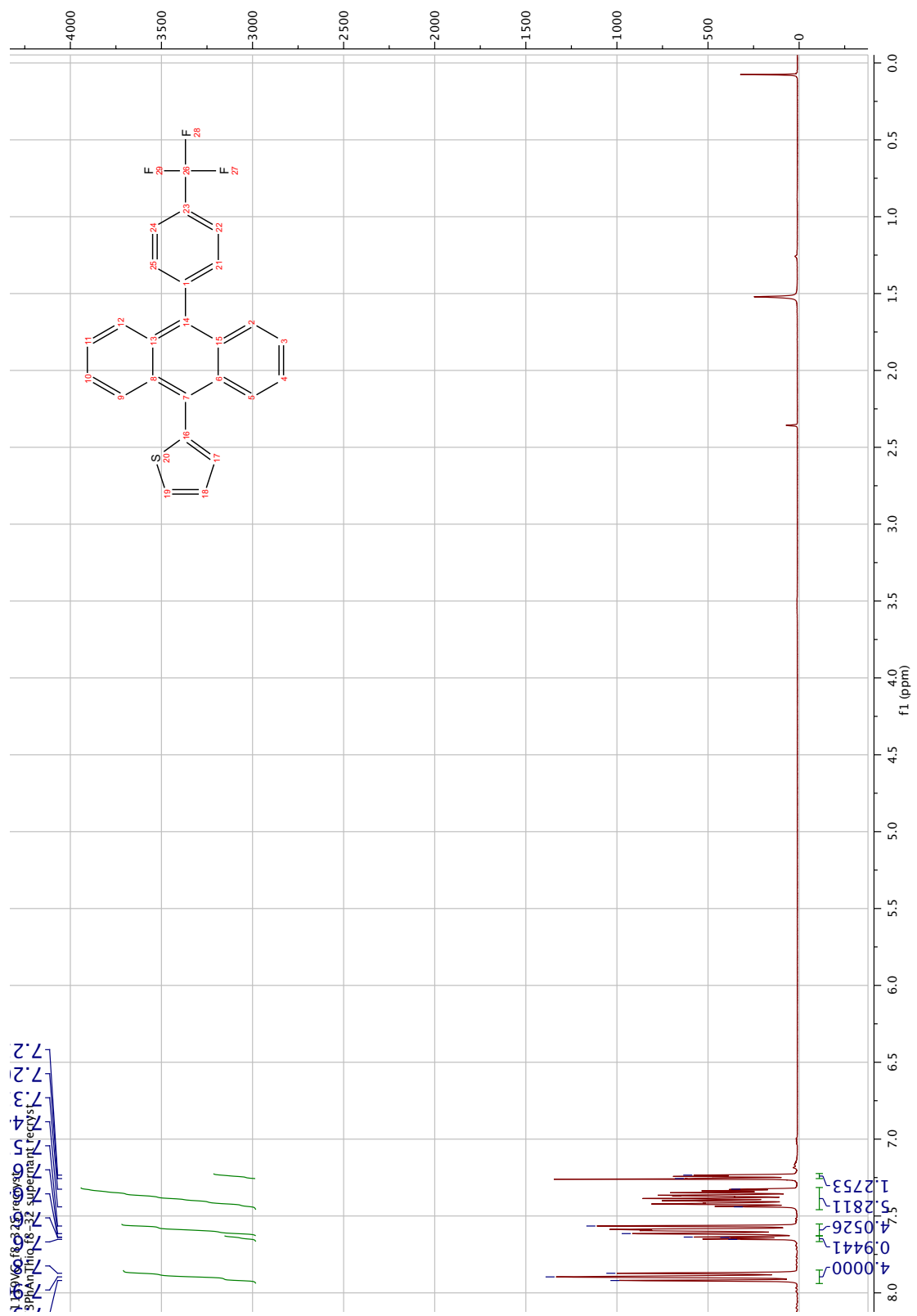


Figure S40:  $^1\text{H}$ -NMR of **9**

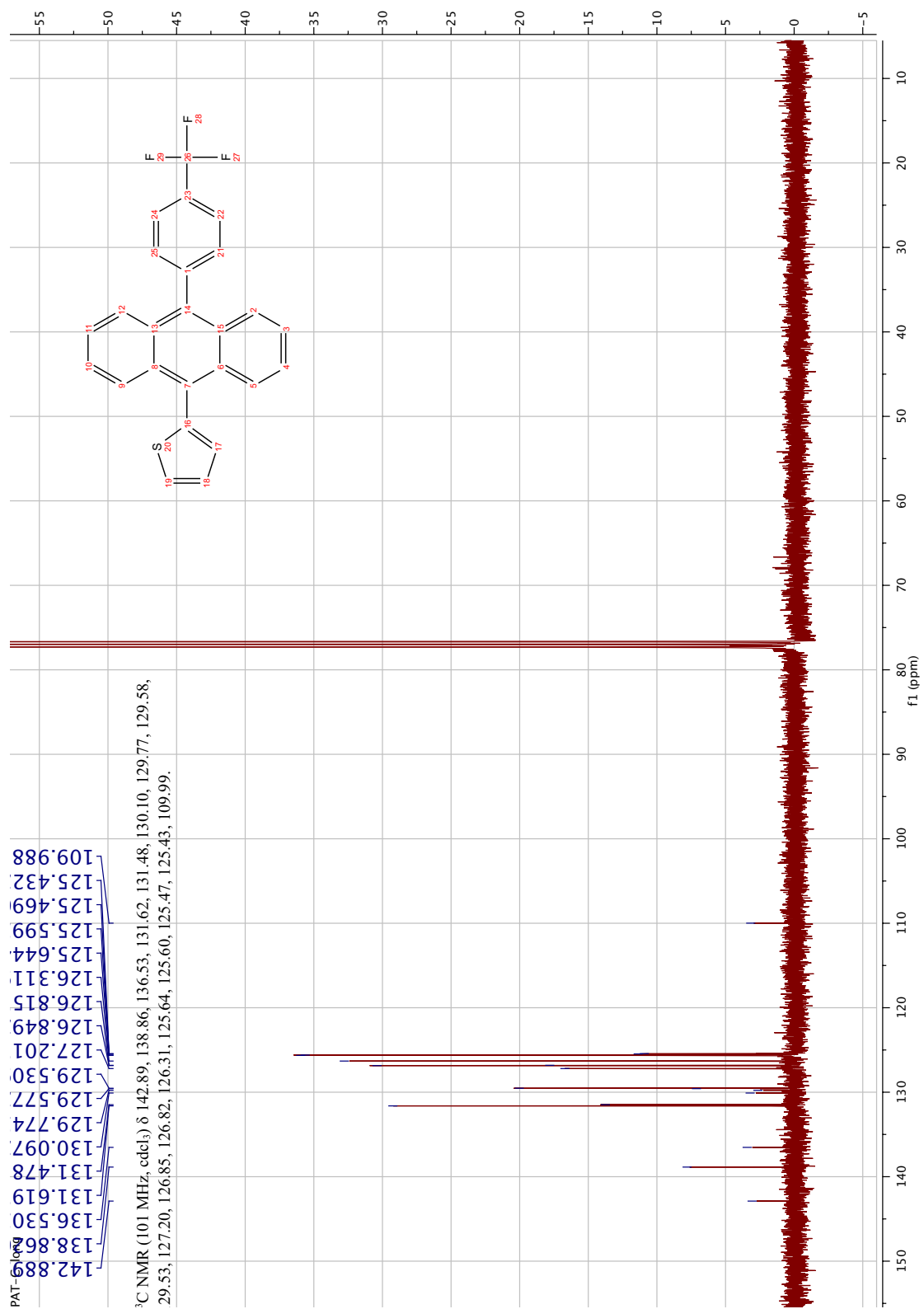


Figure S41:  $^{13}\text{C}$ -NMR of **9**

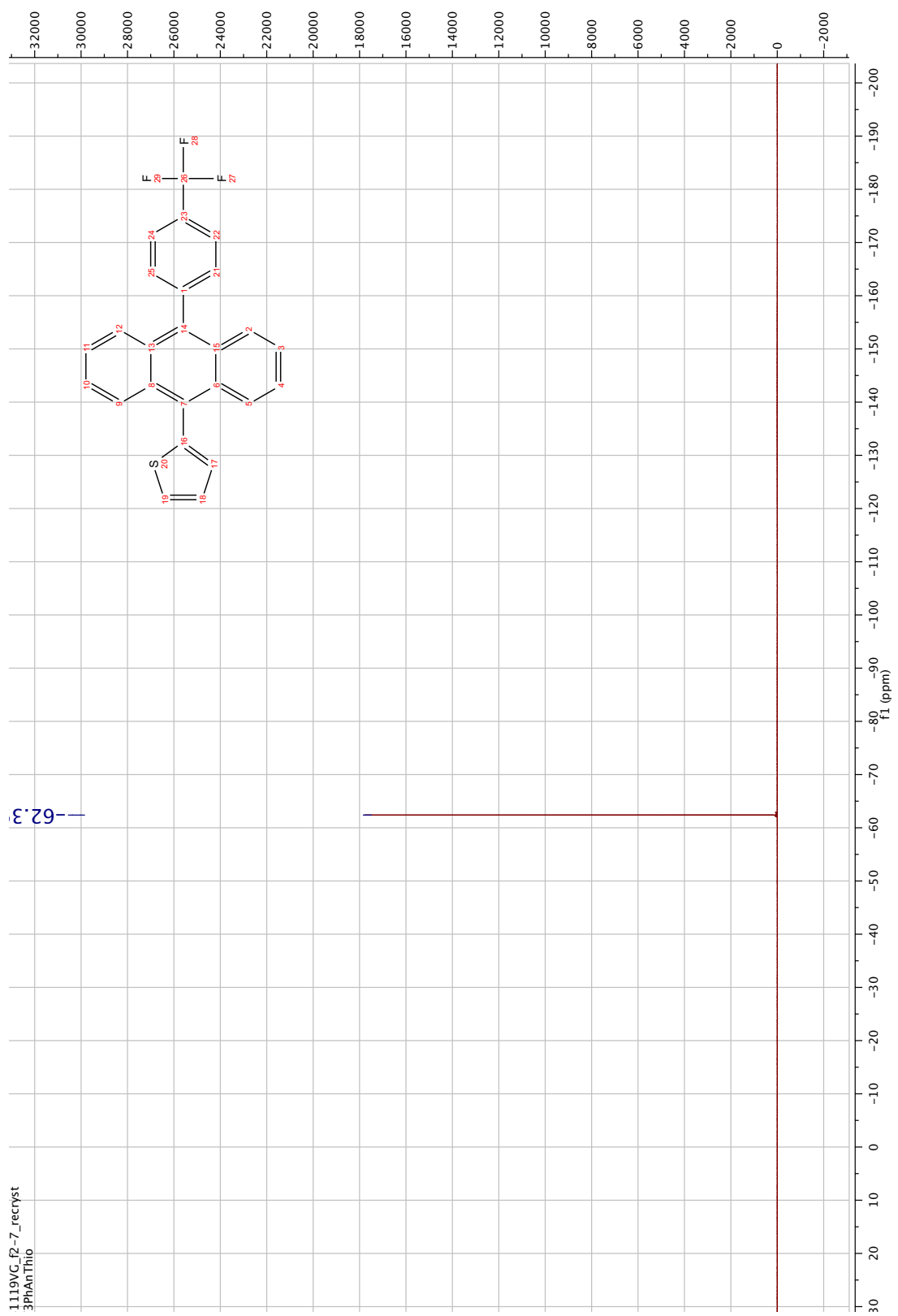


Figure S42: <sup>19</sup>F-NMR of **9**

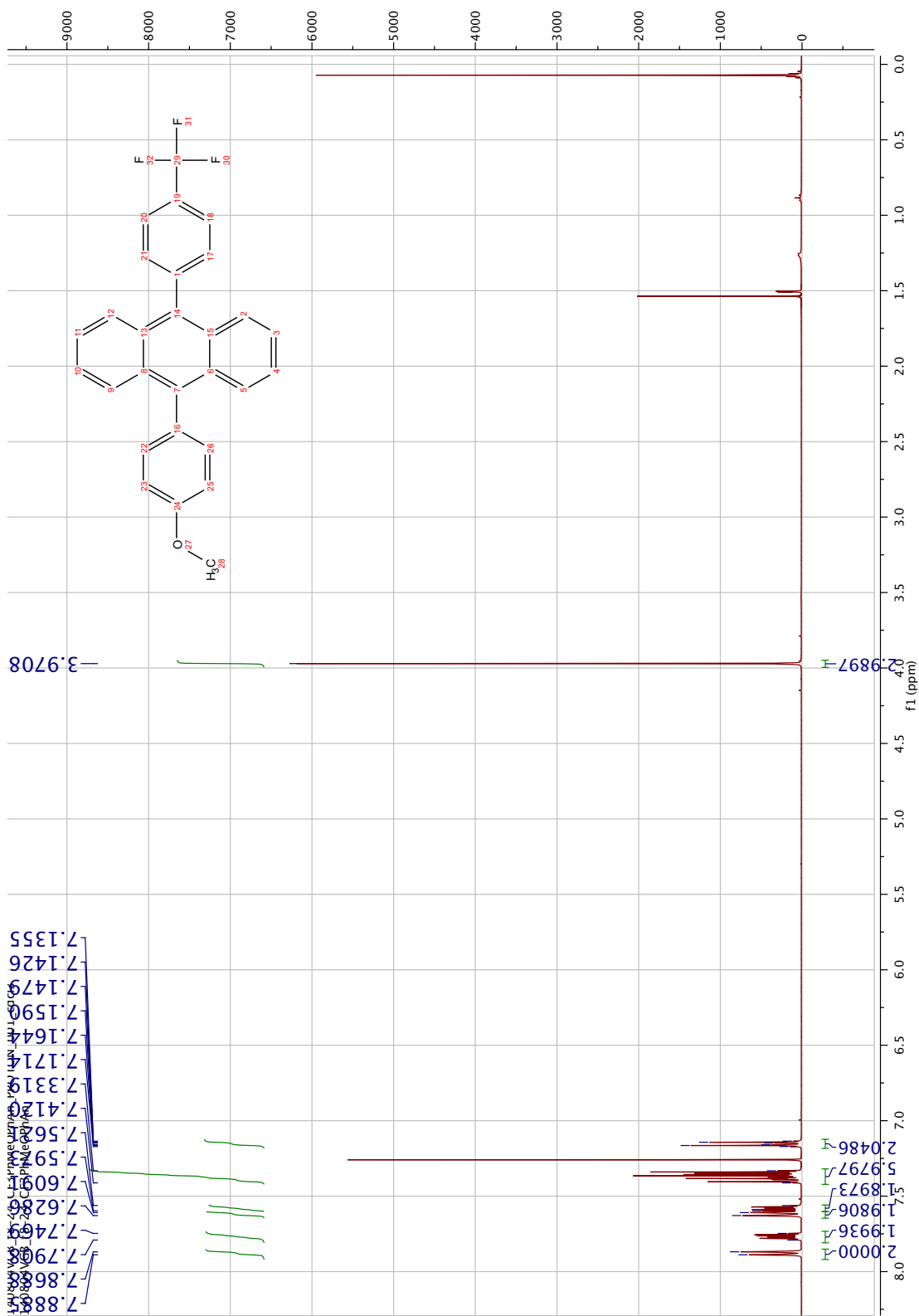


Figure S43:  $^1\text{H}$ -NMR of **10**

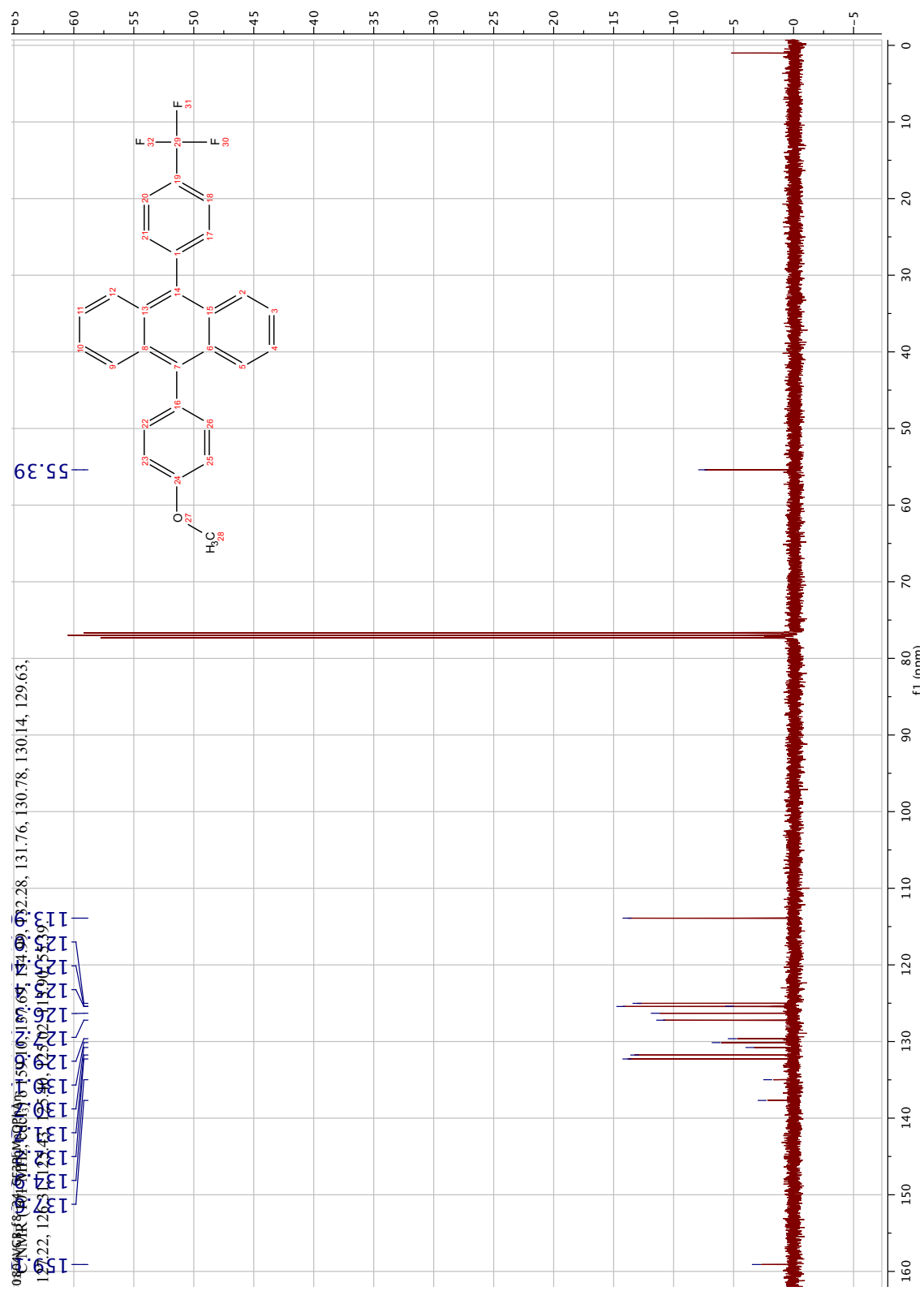


Figure S44:  $^{13}\text{C}$ -NMR of **10**

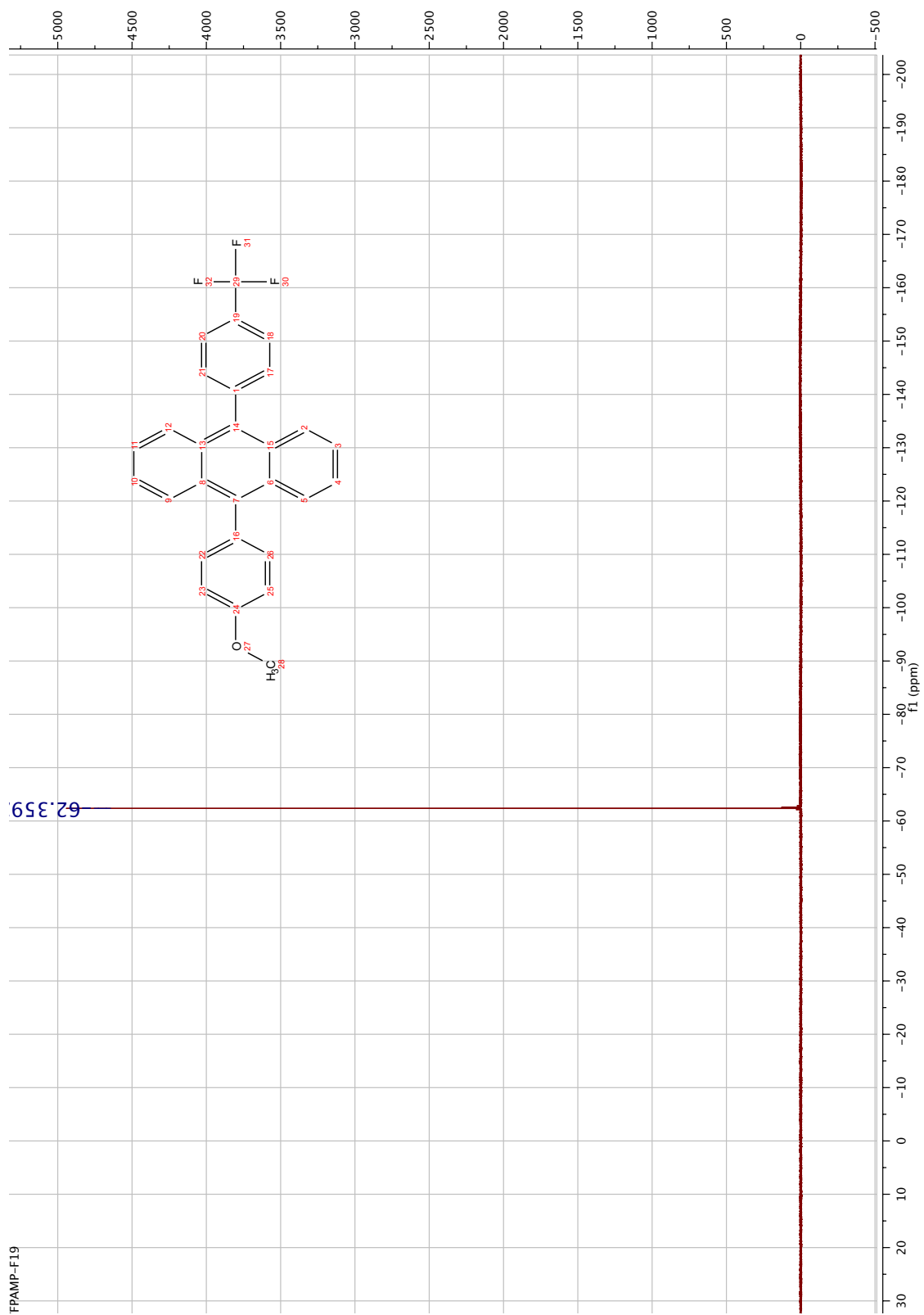


Figure S45:  $^{19}\text{F}$ -NMR of **10**

## References

- (S1) Gray, V.; Dzebo, D.; Abrahamsson, M.; Albinsson, B.; Moth-Poulsen, K. *Phys. Chem. Chem. Phys.* **2014**, *16*, 10345–52.
- (S2) Cheng, Y. Y.; Fückel, B.; Khoury, T.; Clady, R. G. C. R.; Tayebjee, M. J. Y.; Ekins-Daukes, N. J.; Crossley, M. J.; Schmidt, T. W. *J. Phys. Chem. Lett.* **2010**, *1*, 1795–1799.
- (S3) Khnayzer, R. S.; Blumhoff, J.; Harrington, J. A.; Haefele, A.; Deng, F.; Castellano, F. N. *Chem. Commun.* **2012**, *48*, 209.
- (S4) Tilley, A. J.; Robotham, B. E.; Steer, R. P.; Ghiggino, K. P. *Chem. Phys. Lett.* **2015**, *618*, 198–202.